Steel and Composite Structures, *Vol. 22, No. 6 (2016) 1301-1336*
DOI: http://dx.doi.org/10.12989/scs.2016.22.6.1301

Electro-mechanical vibration of nanoshells using consistent size-dependent piezoelectric theory

Narges Ebrahimi [1] and Yaghoub Tadi Beni [*2]

[1] *Mechanical Engineering Department, Shahrekord University, Shahrekord, Iran*
[2] *Faculty of Engineering, Shahrekord University, Shahrekord, Iran*

(*Received July 28, 2016, Revised October 21, 2016, Accepted November 18, 2016*)

Abstract. In this paper, the free vibrations of a short cylindrical nanotube made of piezoelectric material are studied based on the consistent couple stress theory and using the shear deformable cylindrical theory. This new model has only one length scale parameter and can consider the size effects of nanostructures in nanoscale. To model size effects in nanoscale, and considering the nanotube material which is piezoelectric, the consistent couple stress theory is used. First, using Hamilton's principle, the equations of motion and boundary condition of the piezoelectric cylindrical nanoshell are developed. Afterwards, using Navier approach and extended Kantorovich method (EKM), the governing equations of the system with simple-simple (S-S) and clamped-clamped (C-C) supports are solved. Afterwards, the effects of size parameter, geometric parameters (nanoshell length and thickness), and mechanical and electric properties (piezoelectric effect) on nanoshell vibrations are investigated. Results demonstrate that the natural frequency on nanoshell in nanoscale is extremely dependent on nanoshell size. Increase in size parameter, thickness and flexoelectric effect of the material leads to increase in frequency of vibrations. Moreover, increased nanoshell length and diameter leads to decreased vibration frequency.

Keywords: piezoelectric effect; flexoelectric effect; consistent couple-stress theory; electromechanical size-dependent; first order shear deformable theory; extended Kantorovich method

1. Introduction

Today, with the progress of nanoscience, different components in the shape of cylindrical nanoshells are made to be used in nanosystems. One category of the mostly applicable components is carbon nanotubes which serve as the main part of nanodevices and can be simulated as cylindrical shell models. Besides, the cylindrical shell model is used to investigate nanoelectric systems, medical sensors, and drug injection devices by Hummer *et al*. (2001), Gao and Bando (2002), Mattia and Gogotsi (2008). Generally, molecular dynamics (MD) simulation and continuum theory are used to study the behavior of nanosystems by Shayan-Amin *et al*. (2009) and Tsai and Tu (2010). Since the distribution of material is expressed in a completely continuous and uniform fashion in classical continuum theories, and because they are independent of size, these theories are unable to predict size effects in the small dimensions of nanostructure (Chakraverty and Behera 2015). Besides, in view of the fact that maintaining control and conducting

*Corresponding author, Professor, E-mail: tadi@eng.sku.ac.ir

http://www.techno-press.org/?journal=scs&subpage=6 ISSN: 1229-9367 (Print), 1598-6233 (Online)

experiments in nanoscale is expensive and difficult, and because simulation methods such as MD simulation are time-consuming and very expensive, higher order continuum theories including nonlocal theory (Eringen 1983, Liu *et al*. 2016 and Belkorissat *et al*. (2015), couple stress theory (Zeighampour and Tadi Beni 2014, Tadi Beni 2016a, b, c, Mehralian and Tadi Beni 2016), modified couple stress theory (Yang *et al*. 2002, Tadi Beni *et al*. 2014, Mohammadi Dashtaki and Tadi Beni 2014), consistent couple stress theory (Hadjesfandiari and Dargush 2013, Razavi *et al*. 2016), strain gradient theory (Zeighampour and Tadi Beni 2015), modified strain gradient theory (Lam *et al*. 2003, Shojaeian and Tadi Beni 2015) and surface elasticity theory (Gurtin *et al*. 1998) have appealed to researchers.

Tadi Beni *et al*. (2011) investigated the size effect on the pull-in instability of beam type NEMS under van der Waals attraction. Sedighi (2014) developed Size-dependent dynamic pull-in instability of vibrating electrically actuated microbeams by using the strain gradient elasticity theory. He shows that by increasing the actuation voltage parameter, the stable center point loses its stability and coalesces with unstable saddle node. Sedighi and Bozorgmehri (2016) investigated the dynamic instability of free-standing size-dependent nanowires by considering the Casimir force and surface effects. Sedighi *et al*. (2015) is investigated the dynamic instability of functionally graded nano-bridges considering Casimir attraction and electric filed actuation. In this paper, the influences of applied voltage and gradient power of functionally graded materials on the dynamic pull-in voltage and pull-in time of vibrating nano-actuators are explained. Sedighi and Farjam (2016) used new theoretical beam model to investigate the tip charge concentration and rippling phenomenon can substantially affect the electromechanical performance of actuators fabricated from cantilever carbon nanotube. Shojaeian *et al*. (2015) investigated size dependent and pull-in instabilities of initially curved pre-stressed electrostatic nano-bridges.

Asghari *et al*. (2010) developed the nonlocal equations of Timoshenko beam based on modified couple stress theory. They analyzed linear and nonlinear bending and vibration and compared the modified couple stress theory with the classical theory. Tadi Beni and Abadyan (2013) investigated pull-in instability in a nanobeam subjected to torsion using strain gradient theory and compared their findings with those of the couple stress theory. Tadi Beni and Zeighampoor (2014a) modeled cylindrical thin shell based on modified strain gradient theory. In another paper, Tadi Beni and Zeighampoor (2014b) conducted a vibrational analysis of conical shell based on couple stress theory and investigated the effects of nanoshell size and length for different cone angles on the vibration of conical nanoshell.

Sahmani *et al*. (2016) studied the nonlinear buckling and postbuckling characteristics of piezoelectric cylindrical nanoshells subjected to an axial compressive mechanical load and an electrical load in the presence of surface free energy effects.

Civalek (2006) used the discrete singular convolution algorithm for determining the frequencies of the free vibration of laminated conical shells based on Love's first approximation thin shell theory. In addition, Civalek and Gürses (2009) investigated the free vibration of rotating cylindrical shells using discrete singular convolution algorithm.

Akgöz and Civalek (2014) proposed a new non-classical sinusoidal plate model on the basis of modified strain gradient theory. This model takes into account the effects of shear deformation without any shear correction factors and also can capture the size effects due to additional material length scale parameters. Also, Akgöz and Civalek (2015) introduced a new size-dependent beam model on the basis of hyperbolic shear deformation beam and modified strain gradient theory. In addition, Civalek and Akgöz (2013) investigated the free vibration of micro-scaled annular sector and sector shaped graphene located on an elastic matrix via nonlocal elasticity theory.

In recent years, according the studies conducted by Wang *et al*. (2004), piezoelectric materials and their structures as nanowires, nanorings, nanosprings, etc. have attracted the attention of many researchers (Wang 2009, Park *et al*. 2010, Xu and Wang 2011). According to their new and specific electric, mechanical, physical and chemical properties, and due to the couple between mechanical energy and electric energy, piezoelectric nanostructures are used in various kinds of industrial parts in the field of mechanics, aerospace, medical equipment, transportation, communications, nanotransistors, nanodiods, nanocapacitor switches, stepper motors, signal filters, nanogenerators and many other devices in electromechanical and nanoelectromechanical systems. In these applications, due to electric and mechanical loading, the devices are subjected to bending, vibration, buckling (Mehralian *et al*. 2016a, b), etc. Wang *et al*. (2004) observed that the piezoelectric effect of a nanowire made of ZnO material is considerably higher than that of a mass of ZnO material. Chen *et al*. (2006) concluded that the Young's modulus of a nanowire made of ZnO material is dependent on its size. They found out that in a nanowire with a diameter of less than 120nm, decrease in diameter is accompanied by increase in Young's modulus. This study is testimony to the effect of size on mechanical properties of piezoelectric nanostructures. Classical piezoelectric theories which incorporate electromechanical couple between stress and strain with electric polarization are unable to describe materials in micro or nanoscales. Hence, it is necessary to use higher order theories which incorporate the couple between higher order deformations such as strain gradient or mean curvature tensor and polarization field to express the piezoelectric size effect in these scales. Piezoelectric size effect was first discussed by Mishima *et al*. (1997), Shvartsman *et al*. (2002), Buhlmann *et al*. (2002), Cross (2006), Maranganti *et al*. (2006), so that the flexoelectric effect of the material was ultimately established. Recent breakthroughs in nanotechnology necessitate a more advanced model for electromechanical size effect. Hence, piezoelectric size effect theories were developed to incorporate the material length scale into the investigation of the behavior of piezoelectric material. In these theories, the size effect is described using the couple between electric polarizations with higher-order deformations of the continuum. Wang *et al*. (2004) developed a size-dependent piezoelectric theory by applying the effect of rotation gradient within couple stress theory. In that theory, electric polarization depends on rotation gradient. In this connection, the size effect indicator for linear response is recognized with flexoelectric effect, and dielectric polarization depends on strain gradient or curvature strain. However, due to inconsistency, the first step toward consistent electromechanical theories is developing a consistent size-dependent mechanical continuum theory. Recently, Hadjesfandiari and Dargush (2011) have solved the problem of continuum mechanical size effect. Their theory demonstrates that couple stress tensor includes a vector module, and that the moments applied to an object are not distinct from its components. In that theory, stresses are completely clear and the mean curvature tensor which includes the asymmetric part of rotation gradient expresses the degree of deformations. Hadjesfandiari (2013) developed a theory consistent with piezoelectric materials in which electric polarization was dependent on mean curvature tensor.

In other words, Voigt (1887) suggested the presence of couple stress in materials and the Cosserat brothers introduced the first mathematical model to analysis materials with couple stress afterwards. The couple stress theory was later developed for elastic materials by Toupin (1962), Mindlin (1962), and Koiter *et al*. (1964). In these theories, the gradient of the rotation vector is used as a curvature tensor. Due to the presence of body couple in constitutive equations and the consequent difficulty of use of the above theories, these inconsistent theories are called indefinite couple stress theories (Hadjesfandiari and Dargush 2011). Other types of couple stress theories which were developed later with definite boundary conditions and energy conjugacy are in fact not

consistent (Yang *et al*. 2002 and Lazar *et al*. 2005). Based on previous research, Wang *et al*. (2004) developed the size-dependent piezoelectric theory where the rotation gradient effect is expressed based on couple stress theory. It could be argued that the aforementioned size dependent piezoelectric theory is the dielectric polarization which is dependent on curvature strain and in fact, shows that there exists flexoelectric effect for dielectric materials in the isotropic case (Hadjesfandiari 2013 and Tadi Beni 2016a). In this respect, other theories have also been developed (Maranganti *et al*. 2006 and Eliseev 2009), all of which suffer from lack on using of consistent second order gradients of deformation and negligence of couple stress effect (Hadjesfandiari 2013). Based on his previous work (Hadjesfandiari and Dargush 2011), Hadjesfandiari has recently developed the consistent size-dependent piezoelectric theory which is based on the electromechanical formulation and expresses the behavior of continuous materials in the small scale (Hadjesfandiari 2013). Another theory, being used by Ke and Wang (2012), and Ke *et al*. (2012) is the nonlocal theory which has been utilized to model the properties of piezoelectric materials too.

Using higher-order piezoelectric theories, Liang and Shen (2013) expressed the electromechanical couple size effect. They investigated the size effect of a piezoelectric nanowire using Euler-Bernoulli beam model. Ke *et al*. (2012) studied the nonlinear vibrations of a piezoelectric nanobeam based on the nonlocal theory and Timoshenko beam model. Recently, in a paper based on Hadjesfandiari's work, Li *et al*. (2014) investigated the size effect of a three-layer microbeam as well as the electromechanical couple effect for some isotropic materials. Compared to bigger dimensions, the structure of piezoelectric nanomaterials is much more sensitive and important in terms of thermal, electric, and mechanical as well as other chemical and physical properties. Ebrahimiand and Salary (2016) investigated electro-mechanical vibration behavior of piezoelectrically actuated inhomogeneous size-dependent Timoshenko nanobeams by loading a thermal effect. Liu *et al*. (2013) investigated the linear and nonlinear therrmoelectromechanical vibrations of a piezoelectric nanoplate based on Timoshenko beam model and using the nonlocal theory. In another study, based on Love's thin shell theory and nonlocal theory, Ke *et al*. (2014a) modeled an elastic magnetic-electric cylindrical nanoshell. Ke *et al*. (2014b) investigated the thermoelectromechanical vibrations and size effect of a piezoelectric cylindrical nanoshell under different support conditions. In that study, they used the nonlocal theory and thin shell model in their modeling. In general, beam models (the Euler-Bernoulli beam, Timoshenko beam, etc.) are used to simulate electromechanical devices. However, it should be noted that, in more realistic models, it is appropriate to use the cylindrical shell model to model nanotubes. Kheibari and Tadi (2016) investigated the electro-mechanical vibration of single-walled piezoelectric nanotubes using thin shell model. Hoseini *et al*. (2014) studied the free vibration of piezoelectric nanobeams by using the nonlocal theory and applying the effects of surface parameters such as surface stress and surface density. In other studies, Ghorbanpour Arani *et al*. (2012a, b and 2013a, b) analyzed the behavior of boron nitride nanotubes using the nonlocal theory and Timoshenko beam model and shell model. In this study, the aim is to analyze and investigate the behavior of nanotubes, especially piezoelectric nanotubes, by developing a more precise model. In this study, three phenomena are investigated simultaneously and for the first time in the nanostructures, especially nanotubes. First, considering the increasing use of smart materials in nanostructures, this study attempts to investigate the effect of piezoelectric materials in piezoelectric nanotubes. Hence, the piezoelectric effects and mechanical and electric properties of these materials and the vibrations of piezoelectric nanotubes are investigated. Second, in view of the fact that the dependency of material properties of nanostructures on size and dimensions has been proven, this study uses the

consistent couple stress theory which has recently been developed by Hadjesfandiari for piezoelectric materials in order both to model size effects in nanotubes and to dispense with lengthy computations and difficulties related to the atomic theories such as MD simulation and laboratory methods. Third, in order to conduct more precise modeling consistent with nanotube geometry, in this study, the cylindrical shell model is used so that it is closer to the geometry of nanotubes and the effect of system geometry is taken into account precisely. Besides, since the nanotube is assumed short and thick, in this study, the first order shear theory is used to take account of shear deformations along the direction of nanoshell thickness. As can be seen in the literature, previous researchers have commonly used types of beam models to investigate nanotubes and have ignored the effects of nanotube geometry. Except a few studies which have used the shell model to examine carbon nanotubes, other researchers have employed beam models to model nanotubes. A large proportion of research on the modeling of piezoelectric nanostructures has been conducted within beam models and has ignored the material length scale parameter. Hence, it can be argued that the present study is an attempt to develop a more comprehensive and precise model by using the consistent couple stress theory and first order shear model by taking size effect into consideration. In this way, the vibrational behavior of a short piezoelectric nanotube can be described with greater precision compared to previous classical methods. Governing equations of the system, boundary conditions, and initial conditions are determined based on Hamilton's principle. Afterwards, to solve the equations developed, the Navier precise solution and EKM are used in the two simple support and clamped support cases to analyze the free vibration of piezoelectric nanotubes made of BaTiO3 as well as the factors influencing the vibrational behaviors of nanotubes such as material length scale parameter, length , and thickness of shell. Studying the vibrational behavior of such systems can be instrumental in the choice of optimal design parameters of the systems.

2. Size-dependent electromechanical model

In this section, first a summary of the equations of consistent piezoelectric theory based on Hadjesfandiari's work (2013) is presented and then the formulation of a piezoelectric cylindrical nanoshell is developed based on first order shear deformation theory.

2.1 Consistent piezoelectric theory

Hadjesfandiari (2013) has developed a consistent piezoelectric size effect theory to take into consideration the size effect of piezoelectric solids and the electromechanical couple of isotropic materials. That theory is expressed based on couple stress theory, and the asymmetric part of rotation gradient tensor represents the deformations. Based on this theory, electromechanical enthalpy is expressed as follows

$$H = \frac{1}{2}\lambda\varepsilon_{ii}\varepsilon_{jj} + \mu\varepsilon_{ij}\varepsilon_{ij} + 8\mu l^{2}\kappa_i\kappa_i - \frac{1}{2}\varepsilon E_i E_i - 4fE_i\kappa_i \tag{1}$$

The parameters λ and μ have the same meaning as the Lame constants for an isotropic material in Cauchy elasticity 'l is the material length scale parameter, ε is the permittivity, f is the flexoelectric coefficient, ε_{ij} is the strain tensor components, k_i is the mean curvature vector

components and E_i is the electric field vector components.

The strain tensor and rotation tensor are defined in the following way

$$\varepsilon_{ij} = \frac{1}{2}(u_{i,j} + u_{j,i}) \tag{2}$$

$$\omega_{ij} = \frac{1}{2}(u_{i,j} - u_{j,i}) \tag{3}$$

In the Eq. (3), ω_{ij} is the components of rotation tensor and u_i is the components of displacement.

Since the rotation tensor is asymmetric, it can be expressed as a vector with three independent values as displayed in Eq. (4) as follows

$$\omega = \frac{1}{2}\nabla \times u \tag{4}$$

The asymmetric rotation tensor can be defined as the sum of the two distinct symmetric and antisymmetric tensors according to the following equation

$$\omega_{i,j} = k_{ij} + \chi_{ij} \tag{5}$$

where

$$\chi_{ij} = \omega_{(i,j)} = \frac{1}{2}(\nabla\omega + \nabla\omega^T) \tag{6}$$

$$k_{ij} = \omega_{[i,j]} = \frac{1}{2}(\nabla\omega - \nabla\omega^T) \tag{7}$$

Since k_{ij} is the rotation of the rotation vector, it is known as the mean curvature tensor; and because the mean curvature tensor is an antisymmetric tensor, it can be expressed as a vector with three independent values

$$[k_{ij}] = \begin{bmatrix} 0 & k_{12} & k_{13} \\ -k_{12} & 0 & k_{23} \\ -k_{13} & -k_{23} & 0 \end{bmatrix} \tag{8}$$

Therefore, like the rotation vector, it can be rewritten as the following vector

$$k = \frac{1}{2}\nabla \times \omega \tag{9}$$

Besides, based on Griffith theory (1989), the relationship between electric field and electric potential can be expressed as the following equation where φ stands for electric potential.

$$E_i = -\varphi_{,i} \tag{10}$$

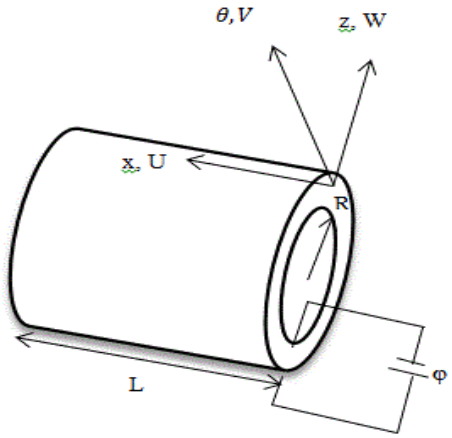

Fig. 1 Schematic configuration of a piezoelectric cylindrical nanoshell

2.2 Displacement and electric fields in cylindrical nanoshell

According to Fig. 1 which illustrates a cylindrical nanoshell with length L, density ρ and thickness h, the displacement field of any arbitrary point in the cylindrical shell based on the first-order shear deformable theory in the x, θ and z direction is as follows

$$u\left(x,\theta,z,t\right)=U\left(x,\theta,t\right)+z\,\Psi_x\left(x,\theta,t\right) \tag{11}$$

$$v\left(x,\theta,z,t\right)=V\left(x,\theta,t\right)+z\,\Psi_\theta\left(x,\theta,t\right) \tag{12}$$

$$w\left(x,\theta,z,t\right)=W\left(x,\theta,t\right) \tag{13}$$

where u,v and w are displacements components of an arbitrary point in the cylindrical shell in terms of x, θ and z coordinates.

Also V (x, θ, t), W (x, θ, t), U (x, θ, t) are three displacement and Ψ_x (x, θ, t) and Ψ_θ(x, θ, t) are rotation around x and θ axes.

Besides, the electric potential applied to the shell based on the equation presented in the references (Ke *et al*. 2014a, b) is assumed as follows

$$\varphi(x,\theta,t,z)=-\cos(\frac{\pi z}{h})\Phi(x,\theta,t)+\frac{2z\,\phi_0}{h} \tag{14}$$

In this equation, Φ is an independent function of z (thickness) and stands for the initial electric voltage applied to the nanoshell.

3. Governing equations of motion and corresponding boundary conditions

By substituting Eqs. (11)-(13) into Eq. (2) in its matrix form and applying the assumption

$\left(1+\frac{z}{R}\right)\approx 1$ from Love's thin shell theory, also substituting the equations developed into Eq. (4), the components of classical and higher order strains and rotation vector are expressed as

$$\begin{aligned}
\varepsilon_{xx} &= \frac{\partial \mathrm{U}}{\partial x}+z\,\frac{\partial \Psi_{\mathrm{x}}}{\partial x}, \\
\varepsilon_{\theta\theta} &= \frac{1}{R}\left[\frac{\partial \mathrm{V}}{\partial \theta}+z\,\frac{\partial \Psi_{\theta}}{\partial \theta}+W\right], \\
\varepsilon_{x\theta} &= \frac{1}{2}\left[\frac{1}{R}\frac{\partial \mathrm{U}}{\partial \theta}+\frac{\partial \mathrm{V}}{\partial x}+\frac{z}{R}\frac{\partial \Psi_{\mathrm{x}}}{\partial \theta}+z\,\frac{\partial \Psi_{\theta}}{\partial x}\right], \\
\varepsilon_{z\theta} &= \frac{1}{2}\left[\Psi_{\theta}+\frac{1}{R}\frac{\partial \mathrm{w}}{\partial \theta}-\frac{\mathrm{V}}{R}\right], \\
\varepsilon_{zx} &= \frac{1}{2}\left[\Psi_{x}+\frac{\partial \mathrm{w}}{\partial x}\right]
\end{aligned} \tag{15}$$

$$\begin{aligned}
\omega_{x} &= \frac{1}{2}\left[\frac{1}{R+z}\frac{\partial W}{\partial \theta}-\frac{1}{R+z}(\mathrm{V}+z\psi_{\theta})-\psi_{\theta}\right], \\
\omega_{\theta} &= \frac{1}{2}\left[\psi_{x}-\frac{\partial W}{\partial x}\right], \\
\omega_{z} &= \frac{1}{2}\left[\frac{\partial V}{\partial x}+z\,\frac{\partial \psi_{\theta}}{\partial x}-\frac{1}{R+z}\left(\frac{\partial U}{\partial \theta}+z\,\frac{\partial \psi_{x}}{\partial \theta}\right)\right]
\end{aligned} \tag{16}$$

The curvature components can be calculated by substituting Eq. (16) into Eq. (9) as

$$\begin{aligned}
\kappa_{x} &= \frac{1}{4}\left[\frac{1}{R+z}\left(\frac{\partial^{2}V}{\partial x\,\partial \theta}+z\,\frac{\partial^{2}\psi_{\theta}}{\partial x\,\partial \theta}-\psi_{x}+\frac{\partial W}{\partial x}\right)-\frac{1}{(R+z)^{2}}\left(\frac{\partial^{2}U}{\partial \theta^{2}}+z\,\frac{\partial^{2}\psi_{x}}{\partial \theta^{2}}\right)\right], \\
\kappa_{\theta} &= \frac{1}{4}\left[\frac{1}{R+z}\left(\frac{\partial^{2}U}{\partial x\,\partial \theta}+z\,\frac{\partial^{2}\psi_{x}}{\partial x\,\partial \theta}\right)-\left(\frac{\partial^{2}V}{\partial x^{2}}+z\,\frac{\partial^{2}\psi_{\theta}}{\partial x^{2}}\right)+\frac{1}{(R+z)^{2}}\left(V+R\psi_{\theta}-\frac{\partial W}{\partial \theta}\right)\right], \\
\kappa_{z} &= \frac{1}{4}\left[\frac{\partial \psi_{x}}{\partial x}-\frac{\partial^{2}W}{\partial x^{2}}+\frac{1}{R+z}\frac{\partial \psi_{\theta}}{\partial \theta}+\frac{1}{(R+z)^{2}}\left(\frac{\partial V}{\partial \theta}+z\,\frac{\partial \psi_{\theta}}{\partial \theta}-\frac{\partial^{2}W}{\partial \theta^{2}}\right)\right]
\end{aligned} \tag{17}$$

The electric field components in terms of x, θ and z coordinates can be calculated by substituting Eq. (14) into Eq. (10) as following

$$\begin{aligned}
E_{x} &= -\frac{\partial \varphi}{\partial x}=\cos\frac{\pi z}{h}\frac{\partial \Phi}{\partial x}, \\
E_{\theta} &= -\frac{1}{R+z}\frac{\partial \varphi}{\partial \theta}=\frac{\cos\frac{\pi z}{h}}{R+z}\frac{\partial \Phi}{\partial \theta},
\end{aligned} \tag{18}$$

$$E_z = -\frac{\partial \varphi}{\partial z} = -\frac{\pi}{h}\sin\frac{\pi z}{h}\Phi - \frac{2\phi_0}{h} \tag{18}$$

Finally by substituting Eqs. (15), (17) and (18) into Eq. (1) the total enthalpy will be given as follows

$$\begin{aligned}
H &= \int_0^{2\pi}\int_0^{L}[N_{xx}]\frac{\partial U}{\partial x}+\left[\frac{N_{x\theta}}{R}\right]\frac{\partial U}{\partial \theta}+[N_{x\theta}]\frac{\partial V}{\partial x}+\left[\frac{N_{\theta\theta}}{R}\right]\frac{\partial V}{\partial \theta}-\left[\frac{Q_{\theta z}}{R}\right]V+[Q_{xz}]\frac{\partial W}{\partial x}\\
&+\left[\frac{Q_{\theta z}}{R}\right]\frac{\partial W}{\partial \theta}+\left[\frac{N_{\theta\theta}}{R}\right]W+[M_{xx}]\frac{\partial \psi_x}{\partial x}+[\frac{M_{x\theta}}{R}]\frac{\partial \psi_x}{\partial \theta}+[M_{x\theta}]\frac{\partial \psi_\theta}{\partial x}+[\frac{M_{\theta\theta}}{R}]\frac{\partial \psi_\theta}{\partial \theta}\\
&+[Q_{\theta z}]\psi_\theta-\frac{1}{2}\varepsilon\{E_xE_x+E_\theta E_\theta+E_zE_z\}-4f\{E_x\kappa_x+E_\theta\kappa_\theta+E_z\kappa_z\}\\
&+8\mu l^2\{\kappa_x\kappa_x+\kappa_\theta\kappa_\theta+\kappa_z\kappa_z\}Rdxd\theta\\
&=\int_0^{2\pi}\int_0^{L}[N_{xx}]\frac{\partial U}{\partial x}+\left[\frac{N_{x\theta}}{R}\right]\frac{\partial U}{\partial \theta}+[N_{x\theta}]\frac{\partial V}{\partial x}+\left[\frac{N_{\theta\theta}}{R}\right]\frac{\partial V}{\partial \theta}-\left[\frac{Q_{\theta z}}{R}\right]V+[Q_{xz}]\frac{\partial W}{\partial x}\\
&+\left[\frac{Q_{\theta z}}{R}\right]\frac{\partial W}{\partial \theta}+\left[\frac{N_{\theta\theta}}{R}\right]W+[M_{xx}]\frac{\partial \psi_x}{\partial x}+[\frac{M_{x\theta}}{R}]\frac{\partial \psi_x}{\partial \theta}+[M_{x\theta}]\frac{\partial \psi_\theta}{\partial x}+[\frac{M_{\theta\theta}}{R}]\frac{\partial \psi_\theta}{\partial \theta}\\
&+[Q_{\theta z}]\psi_\theta-\frac{1}{2}\varepsilon\left[\cos^2\frac{\pi z}{h}?\frac{\partial\Phi}{\partial x})^2+\frac{\cos^2\frac{\pi z}{h}}{R^2(1+\frac{z}{R})^2}?\frac{\partial\Phi}{\partial\theta})^2+(-\frac{\pi}{h})^2\sin^2\frac{\pi z}{h}\Phi^2\right]\\
&-f\left\{\cos\frac{\pi z}{h}?\frac{\partial\Phi}{\partial x}\left[\frac{1}{R+z}\left(\frac{\partial^2 V}{\partial x\,\partial\theta}+z\frac{\partial^2\psi_\theta}{\partial x\,\partial\theta}-\psi_x+\frac{\partial W}{\partial x}\right)-\frac{1}{(R+z)^2}\left(\frac{\partial^2 U}{\partial\theta^2}+z\frac{\partial^2\psi_x}{\partial\theta^2}\right)\right]\right.\\
&+\frac{\cos\frac{\pi z}{h}}{R+z}\frac{\partial\Phi}{\partial\theta}+\frac{\cos\frac{\pi z}{h}}{R+z}\frac{\partial\Phi}{\partial\theta}\left[\frac{1}{R+z}\left(\frac{\partial^2 U}{\partial x\,\partial\theta}+z\frac{\partial^2\psi_x}{\partial x\,\partial\theta}\right)-\left(\frac{\partial^2 V}{\partial x^2}+z\frac{\partial^2\psi_\theta}{\partial x^2}\right)\right.\\
&\left.\left.+\frac{1}{(R+z)^2}\left(V+R\psi_\theta-\frac{\partial W}{\partial\theta}\right)\right]-\frac{\pi}{h}\sin\frac{\pi z}{h}\Phi\left[\frac{\partial\psi_x}{\partial x}-\frac{\partial^2 W}{\partial x^2}+\frac{1}{R+z}\frac{\partial\psi_\theta}{\partial\theta}\right.\right.\\
&\left.\left.+\frac{1}{(R+z)^2}\left(\frac{\partial V}{\partial\theta}+z\frac{\partial\psi_\theta}{\partial\theta}-\frac{\partial^2 W}{\partial\theta^2}\right)\right]+\frac{\mu l^2}{2}\left\{\left[\frac{1}{R+z}\left(\frac{\partial^2 V}{\partial x\,\partial\theta}+z\frac{\partial^2\psi_\theta}{\partial x\,\partial\theta}-\psi_x+\frac{\partial W}{\partial x}\right)\right.\right.\\
&\left.-\frac{1}{(R+z)^2}\left(\frac{\partial^2 U}{\partial\theta^2}+z\frac{\partial^2\psi_x}{\partial\theta^2}\right)\right]^2+\left[\frac{1}{R+z}\left(\frac{\partial^2 U}{\partial x\,\partial\theta}+z\frac{\partial^2\psi_x}{\partial x\,\partial\theta}\right)-\left(\frac{\partial^2 V}{\partial x^2}+z\frac{\partial^2\psi_\theta}{\partial x^2}\right)\right.\\
&+\frac{1}{(R+z)^2}\left(V+R\psi_\theta-\frac{\partial W}{\partial\theta}\right)\Big]^2+\left[\frac{\partial\psi_x}{\partial x}-\frac{\partial^2 W}{\partial x^2}+\frac{1}{R+z}\frac{\partial\psi_\theta}{\partial\theta}\right.\\
&\left.\left.\left.+\frac{1}{(R+z)^2}(\frac{\partial V}{\partial\theta}+z\frac{\partial\psi_\theta}{\partial\theta}-\frac{\partial^2 W}{\partial\theta^2})\right]^2\right\}Rdxd\theta
\end{aligned} \tag{19}$$

In the above equations, classical forces and moments are written as follows

$$M_{ij} = \int_{-\frac{h}{2}}^{\frac{h}{2}} \sigma_{ij} z dz \quad , \quad N_{ii} = \int_{-\frac{h}{2}}^{\frac{h}{2}} \sigma_{ij} dz \tag{20}$$

Also in all equations is considered the assumption of Love's thin shell theory $\left(\left(1+\frac{z}{R}\right)\approx 1\right)$.

The kinetic energy for cylindrical shell is stated as follows

$$T = \frac{1}{2}\rho \int_0^{2\pi}\int_0^{L}\int_{-\frac{h}{2}}^{\frac{h}{2}} \left\{ (\frac{\partial U}{\partial t} + z\ \frac{\partial \psi_x}{\partial t})^2 + (\frac{\partial V}{\partial t} + z\ \frac{\partial \psi_\theta}{\partial t})^2 + (\frac{\partial W}{\partial t})^2 \right\} R dz dx d\theta \tag{21}$$

The mechanical work is defined as the summation of the work of distributed forces and tractions applied in boundaries.

$$W_{mech} = W_d + W_b \tag{22}$$

The work of external mechanical forces on cylindrical shell is expressed as

$$w_d = \int_x \int_\theta (f_u U + f_v V + f_w W) R dx d\theta \tag{23}$$

where f_u, f_v and $f_w$are the volume distributed forces.

The work of external forces on the cylindrical nanoshell is expressed as the following

$$\begin{aligned} w_b = \int_\theta \Big\{ & \overline{N_x}^{u} U + \overline{N_x}^{v} V + \hat{P}_x^{vh} \frac{\partial V}{\partial x} + \overline{N_x}^{w} W + \overline{M_x}^{wh} \frac{\partial W}{\partial x} + \overline{M_{xx}}^{\psi} \psi_x \\ & + \overline{M_{x\theta}}^{\psi} \psi_\theta + \overline{R_x^{\psi}} \frac{\partial \psi_\theta}{\partial x} \Big\} R d\theta \Big|_0^L + \Big\{ \int_x \overline{N_\theta}^{u} U + P_\theta^{uh} \frac{\partial U}{\partial \theta} + \overline{N}^{v}_{\theta} V + \overline{N}^{w}_{\theta} W + \overline{M}^{wh}_{\theta} \frac{\partial W}{\partial \theta} \\ & + \overline{M}^{\psi}_{\theta\theta} \psi_\theta + \overline{M}^{\psi}_{\theta x} \psi_x \Big\} R dx \Big|_0^{\theta_1} \end{aligned} \tag{24}$$

The piezoelectric work of the system is expressed as

$$W_{elec} = \int \rho_e\ \varphi dV \tag{25}$$

The total work is the summation of the mechanical work and piezoelectric work.

$$W_{total} = W_{elec} + W_{mech} \tag{26}$$

Then the Hamilton's principle are used as following

$$\int_{t_1}^{t_2}\left(\delta T-\delta H+\delta W_{total}\right)dt=0 \tag{27}$$

Now, by substituting the values of enthalpy, kinetic energy and the work of external forces of the system from the above equations into Eq. (27) and calculating the variation, the equations of motion are determined as follows

$$\begin{aligned}&\mathrm{A}_1\frac{\partial^2 U}{\partial x^2}+\mathrm{A}_2\frac{\partial^4 U}{\partial x^2\partial\theta^2}+\mathrm{A}_3\frac{\partial^2 U}{\partial\theta^2}+\mathrm{A}_4\frac{\partial^4 U}{\partial\theta^4}+\mathrm{A}_5\frac{\partial^4 V}{\partial x^3\partial\theta}+\mathrm{A}_6\frac{\partial^2 V}{\partial x\,\partial\theta}+\mathrm{A}_7\frac{\partial^4 V}{\partial x\,\partial\theta^3}\\&+\mathrm{A}_8\frac{\partial W}{\partial x}+\mathrm{A}_9\frac{\partial^3 W}{\partial x\,\partial\theta^2}+\mathrm{A}_{10}\frac{\partial^2\psi_\theta}{\partial x\,\partial\theta}+\mathrm{A}_{11}\frac{\partial^2\psi_x}{\partial\theta^2}-f_u+\rho h\frac{\partial^2 U}{\partial t^2}=0\end{aligned} \tag{28}$$

$$\begin{aligned}&B_1\frac{\partial^4 V}{\partial x^4}+B_2\frac{\partial^2 V}{\partial x^2}+B_3\frac{\partial^2 V}{\partial\theta^2}+B_4\frac{\partial^4 V}{\partial x^2\partial\theta^2}+B_5V+B_6\frac{\partial^4 U}{\partial x^3\partial\theta}+B_7\frac{\partial^4 U}{\partial x\,\partial\theta^3}+B_8\frac{\partial^2 U}{\partial x\,\partial\theta}\\&+B_9\frac{\partial^3 W}{\partial x^2\partial\theta}+B_{10}\frac{\partial^3 W}{\partial\theta^3}+B_{11}\frac{\partial W}{\partial\theta}+B_{12}\frac{\partial^2\psi_x}{\partial\theta\partial x}+B_{13}\frac{\partial^2\psi_\theta}{\partial\theta^2}+\mathrm{B}_{14}\psi_\theta+\mathrm{B}_{15}\frac{\partial^2\psi_\theta}{\partial x^2}\\&+\mathrm{B}_{16}\frac{\partial\Phi}{\partial\theta}-f_v+\rho h\frac{\partial^2 V}{\partial t^2}=0\end{aligned} \tag{29}$$

$$\begin{aligned}&C_1\frac{\partial^4 W}{\partial x^4}+C_2\frac{\partial^2 W}{\partial x^2}+C_3\frac{\partial^4 W}{\partial x^2\partial\theta^2}+C_4\frac{\partial^4 W}{\partial\theta^4}+C_5\frac{\partial^2 W}{\partial\theta^2}+C_6W+C_7\frac{\partial U}{\partial x}+C_8\frac{\partial^3 U}{\partial x\,\partial\theta^2}\\&+C_9\frac{\partial^3 V}{\partial x^2\partial\theta}+C_{10}\frac{\partial V}{\partial\theta}+C_{11}\frac{\partial^3 V}{\partial\theta^3}+C_{12}\frac{\partial^3\psi_x}{\partial\theta^2\partial x}+C_{13}\frac{\partial^3\psi_x}{\partial x^3}+C_{14}\frac{\partial\psi_x}{\partial x}+C_{15}\frac{\partial^3\psi_\theta}{\partial\theta^3}\\&+C_{16}\frac{\partial\psi_\theta}{\partial\theta}+C_{17}\frac{\partial^3\psi_\theta}{\partial x^2\partial\theta}+C_{18}\frac{\partial^2\Phi}{\partial x^2}+C_{19}\frac{\partial^2\Phi}{\partial\theta^2}-f_w+\rho h\frac{\partial^2 W}{\partial t^2}=0\end{aligned} \tag{30}$$

$$\begin{aligned}&D_1\frac{\partial^2\psi_x}{\partial x^2}+D_2\frac{\partial^4\psi_x}{\partial x^2\partial\theta^2}+D_3\frac{\partial^4\psi_x}{\partial\theta^4}+D_4\frac{\partial^2\psi_x}{\partial\theta^2}+D_5\psi_x+D_6\frac{\partial^2\psi_\theta}{\partial x\,\partial\theta}+D_7\frac{\partial^4\psi_\theta}{\partial x\,\partial\theta^3}\\&+D_8\frac{\partial^4\psi_\theta}{\partial x^3\partial\theta}+D_9\frac{\partial^2 U}{\partial\theta^2}+D_{10}\frac{\partial^2 V}{\partial x\,\partial\theta}+D_{11}\frac{\partial^3 W}{\partial x^3}+D_{12}\frac{\partial^3 W}{\partial\theta^2\partial x}+D_{13}\frac{\partial W}{\partial x}\\&+D_{14}\frac{\partial\Phi}{\partial x}+\frac{\rho h^3}{12}\frac{\partial^2\psi_x}{\partial t^2}=0\end{aligned} \tag{31}$$

$$\begin{aligned}&E_1\frac{\partial^4\psi_\theta}{\partial x^4}+E_2\frac{\partial^2\psi_\theta}{\partial x^2}+E_3\frac{\partial^4\psi_\theta}{\partial x^2\partial\theta^2}+E_4\frac{\partial^2\psi_\theta}{\partial\theta^2}+E_5\psi_\theta+E_6\frac{\partial^2\psi_x}{\partial x\,\partial\theta}+E_7\frac{\partial^4\psi_x}{\partial x\,\partial\theta^3}\\&+E_8\frac{\partial^4\psi_x}{\partial x^3\partial\theta}+E_9\frac{\partial^2 U}{\partial x\,\partial\theta}+E_{10}\frac{\partial^2 V}{\partial x^2}+E_{11}\frac{\partial^2 V}{\partial\theta^2}+E_{12}V+E_{13}\frac{\partial^3 W}{\partial\theta\partial x^2}+E_{14}\frac{\partial^3 W}{\partial\theta^3}\\&+E_{15}\frac{\partial W}{\partial\theta}+E_{16}\frac{\partial\Phi}{\partial\theta}+\frac{\rho h^3}{12}\frac{\partial^2\psi_\theta}{\partial t^2}=0\end{aligned} \tag{32}$$

$$F_1\frac{\partial^2\Phi}{\partial x^2}+F_2\frac{\partial^2\Phi}{\partial\theta^2}+F_3\Phi+F_4\frac{\partial V}{\partial\theta}+F_5\frac{\partial\psi_x}{\partial x}+F_6\frac{\partial\psi_\theta}{\partial\theta}+F_7\frac{\partial^2 W}{\partial x^2}+F_8\frac{\partial^2 W}{\partial\theta^2}-\rho_e=0 \tag{33}$$

The constant coefficients $A_1 - A_{12}$, $B_1 - B_{17}$, $C_1 - C_{19}$, $D_1 - D_{14}$, $E_1 - E_{16}$, $F_1 - F_8$ of Eqs. (28)-(33) are presented in Appendix A.

The boundary conditions in cylindrical shell for edges with x = constant are as follows

$$\int_\theta\left\{a^1{}_1\frac{\partial U}{\partial x}+a^1{}_2\frac{\partial^3 U}{\partial x\,\partial\theta^2}+a^1{}_3\frac{\partial^3 V}{\partial x^2\partial\theta}+a^1{}_4\frac{\partial V}{\partial\theta}+a^1{}_5 W+a^1{}_6\frac{\partial^2 W}{\partial\theta^2}+a^1{}_7\frac{\partial\psi_\theta}{\partial\theta}+a_8^1\frac{\partial^2\Phi}{\partial\theta^2}+\overline{N_x}^u\right\}d\theta\Big|_{x=0,L}=0 \quad \text{or} \quad \delta U\big|_{x=0,L}=0 \tag{34}$$

$$\int_\theta\left\{b^1{}_1\frac{\partial^3 V}{\partial x^3}+b^1{}_2\frac{\partial V}{\partial x}+b^1{}_3\frac{\partial^3 V}{\partial x\,\partial\theta^2}+b^1_4\frac{\partial^3 U}{\partial x^2\partial\theta}+b^1{}_5\frac{\partial^3 U}{\partial\theta^3}+b^1{}_6\frac{\partial U}{\partial\theta}+b^1{}_7\frac{\partial^2 W}{\partial x\,\partial\theta}+b^1{}_8\frac{\partial\psi_\theta}{\partial\theta}+b^1{}_9\frac{\partial\psi_\theta}{\partial x}+\overline{N_x}^v\right\}d\theta\Big|_{x=0,L}=0 \quad \text{or} \quad \delta V\big|_{x=0,L}=0 \tag{35}$$

$$\int_\theta\left\{b^1_{10}\frac{\partial^2 V}{\partial x^2}+b^1_{11}V+b^1_{12}\frac{\partial^2 U}{\partial x\,\partial\theta}+b^1_{13}\frac{\partial W}{\partial\theta}+b^1_{14}\psi_\theta+b^1_{15}\frac{\partial\Phi}{\partial\theta}+\hat{P}_x^{vh}\right\}d\theta\Big|_{x=0,L}=0 \quad \text{or} \quad \delta\left(\frac{\partial V}{\partial x}\right)\Big|_{x=0,L}=0 \tag{36}$$

$$\int_\theta\left\{c^1{}_1\frac{\partial^3 W}{\partial x^3}+c^1{}_2\frac{\partial W}{\partial x}+c^1{}_3\frac{\partial^3 W}{\partial x\,\partial\theta^2}+c^1_4\frac{\partial^2 U}{\partial\theta^2}+c^1{}_5\frac{\partial^2 V}{\partial x\,\partial\theta}+c^1{}_6\psi_x+c^1{}_7\frac{\partial^2\psi_x}{\partial x^2}+c^1{}_8\frac{\partial^2\psi_\theta}{\partial\theta\partial x}+c_9^1\frac{\partial\Phi}{\partial x}+\overline{N_x}^w\right\}d\theta\Big|_{x=0,L}=0 \quad \text{or} \quad \delta W\big|_{x=0,L}=0 \tag{37}$$

$$\int_\theta\left\{c^1_{10}\frac{\partial^2 W}{\partial x^2}+c^1_{11}\frac{\partial^2 W}{\partial\theta^2}+c^1_{12}\frac{\partial\psi_\theta}{\partial\theta}+c^1_{13}\frac{\partial\psi_x}{\partial x}+c^1_{14}\frac{\partial V}{\partial\theta}+\overline{M_x}^{wh}\right\}d\theta\Big|_{x=0,L}=0 \quad \text{or} \quad \delta\left(\frac{\partial W}{\partial x}\right)\Big|_{x=0,L}=0 \tag{38}$$

$$\int_\theta\left\{d^1{}_1\frac{\partial^2 W}{\partial x^2}+d^1{}_2\frac{\partial^2 W}{\partial\theta^2}+d^1{}_3\frac{\partial\psi_\theta}{\partial\theta}+d^1_4\frac{\partial\psi_x}{\partial x}+d^1{}_5\frac{\partial V}{\partial\theta}+d^1{}_6\frac{\partial^3\psi_\theta}{\partial\theta\partial x^2}+d^1{}_7\frac{\partial^3\psi_x}{\partial\theta^2\partial x}+\overline{M_{xx}}^{\psi}\right\}d\theta\Big|_{x=0,L}=0 \quad \text{or} \quad \delta\psi_x\big|_{x=0,L}=0 \tag{39}$$

$$\int_{\theta}\left\{e^{1}_{1}\frac{\partial\psi_{\theta}}{\partial x}+e^{1}_{2}\frac{\partial\psi_{x}}{\partial\theta}+e^{1}_{3}\frac{\partial^{3}\psi_{x}}{\partial\theta^{3}}+e^{1}_{4}\frac{\partial^{3}\psi_{x}}{\partial\theta\partial x^{2}}+e^{1}_{5}\frac{\partial^{3}\psi_{\theta}}{\partial x^{3}}+e^{1}_{6}\frac{\partial^{3}\psi_{\theta}}{\partial\theta^{2}\partial x}+\overline{M}^{\psi}_{x\theta}\right\}d\theta\Big|_{x=0,L}=0 \quad \text{or} \quad \delta\psi_{\theta}\big|_{x=0,L}=0 \tag{40}$$

$$\int_{\theta}\left\{e^{1}_{7}\frac{\partial^{2}\psi_{x}}{\partial x\,\partial\theta}+e^{1}_{8}\frac{\partial^{2}\psi_{\theta}}{\partial x^{2}}+\hat{R}^{h}_{x}\right\}d\theta\Big|_{x=0,L}=0 \quad \text{or} \quad \delta\left(\frac{\partial\psi_{\theta}}{\partial x}\right)\Big|_{x=0,L}=0 \tag{41}$$

$$\int_{\theta}\left\{f_{1}^{1}\frac{\partial\Phi}{\partial x}+f_{2}^{1}\frac{\partial^{2}V}{\partial x\,\partial\theta}+f_{3}^{1}\frac{\partial^{2}U}{\partial\theta^{2}}+f_{4}^{1}\frac{\partial W}{\partial x}+f_{5}^{1}\psi_{x}\right\}d\theta\Big|_{x=0,L}=0 \quad \text{or} \quad \delta\Phi\big|_{x=0,L}=0 \tag{42}$$

The boundary conditions for edges with θ = constant are as follows

$$\int_{x}\left\{a^{2}_{1}\frac{\partial^{3}U}{\partial x^{3}}+a^{2}_{2}\frac{\partial U}{\partial\theta}+a^{2}_{3}\frac{\partial^{3}U}{\partial x^{2}\partial\theta}+a^{2}_{4}\frac{\partial^{3}V}{\partial x\,\partial\theta^{2}}+a^{2}_{5}\frac{\partial V}{\partial x}+a^{2}_{6}\frac{\partial^{3}V}{\partial x^{3}}+a^{1}_{7}\frac{\partial^{2}W}{\partial x\,\partial\theta}+a^{2}_{8}\frac{\partial\psi_{x}}{\partial\theta}+a^{2}_{9}\frac{\partial\psi_{\theta}}{\partial x}+\overline{N}^{u}_{\theta}\right\}dx\Big|_{\theta=0,\theta_{0}}=0 \quad \text{or} \quad \delta U\big|_{\theta=0,\theta_{0}}=0 \tag{43}$$

$$\int_{x}\left\{a^{2}_{10}\frac{\partial^{2}U}{\partial\theta^{2}}+a^{2}_{11}\frac{\partial^{2}V}{\partial x\,\partial\theta}+a^{2}_{12}\frac{\partial W}{\partial x}+a^{2}_{13}\psi_{x}+a^{2}_{14}\frac{\partial\Phi}{\partial x}+\hat{P}^{uh}_{\theta}\right\}dx\Big|_{\theta=0,\theta_{0}}=0 \quad \text{or} \quad \delta\left(\frac{\partial U}{\partial\theta}\right)\Big|_{\theta=0,\theta_{0}}=0 \tag{44}$$

$$\int_{x}\left\{b^{2}_{1}\frac{\partial V}{\partial\theta}+b^{2}_{2}\frac{\partial^{3}V}{\partial x^{2}\partial\theta}+b^{2}_{3}\frac{\partial^{3}U}{\partial x\,\partial\theta^{2}}+b^{2}_{4}\frac{\partial U}{\partial x}+b^{2}_{5}W+b^{2}_{6}\frac{\partial^{2}W}{\partial\theta^{2}}+b^{2}_{7}\frac{\partial\psi_{\theta}}{\partial\theta}+b^{2}_{8}\frac{\partial\psi_{x}}{\partial x}+b^{2}_{9}\frac{\partial^{2}W}{\partial x^{2}}+b^{2}_{10}\frac{\partial^{3}W}{\partial x^{2}\partial\theta}+b^{2}_{11}\frac{\partial^{2}\Phi}{\partial x^{2}}+\overline{N}^{v}_{\theta}\right\}dx\Big|_{\theta=0,\theta_{0}}=0 \quad \text{or} \quad \delta V\big|_{\theta=0,\theta_{0}}=0 \tag{45}$$

$$\int_{x}\left\{c^{2}_{1}\frac{\partial^{3}W}{\partial x^{3}}+c^{2}_{2}\frac{\partial W}{\partial\theta}+c^{2}_{3}\frac{\partial^{3}W}{\partial x^{2}\partial\theta}+c^{2}_{4}\frac{\partial^{2}V}{\partial x^{2}}+c^{2}_{5}\frac{\partial^{2}V}{\partial\theta^{2}}+c^{2}_{6}V+\frac{\partial^{3}V}{\partial x^{3}}+c^{1}_{7}\frac{\partial^{2}U}{\partial x\,\partial\theta}+c^{2}_{8}\frac{\partial^{2}\psi_{x}}{\partial x\,\partial\theta}+c^{2}_{9}\psi_{\theta}+c^{2}_{10}\frac{\partial^{2}\psi_{\theta}}{\partial\theta^{2}}+c^{2}_{11}\frac{\partial\Phi}{\partial\theta}+\overline{N}^{w}_{\theta}\right\}dx\Big|_{\theta=0,\theta_{0}}=0 \quad \text{or} \quad \delta W\big|_{\theta=0,\theta_{0}}=0 \tag{46}$$

$$\int_{x}\left\{c^{2}_{12}\frac{\partial V}{\partial\theta}+c^{2}_{13}\frac{\partial^{2}W}{\partial x^{2}}+c^{2}_{14}\frac{\partial^{2}W}{\partial\theta^{2}}+c^{2}_{15}\frac{\partial\psi_{x}}{\partial x}+c^{2}_{16}\frac{\partial\psi_{\theta}}{\partial\theta}+\overline{M}^{wh}_{\theta}\right\}dx\Big|_{\theta=0,\theta_{0}}=0 \tag{47}$$

$$\text{or} \qquad \delta\left(\frac{\partial W}{\partial \theta}\right)\Big|_{\theta=0,\theta_0} = 0 \tag{47}$$

$$\int_x \left\{ d^{2}_{1}\frac{\partial^3 \psi_x}{\partial \theta^3} + d^{2}_{2}\frac{\partial \psi_\theta}{\partial x} + d^{2}_{3}\frac{\partial^3 \psi_\theta}{\partial x\,\partial \theta^2} + d^{2}_{4}\frac{\partial^3 \psi_\theta}{\partial x^3} + d^{2}_{5}\frac{\partial^3 \psi_x}{\partial x^2 \partial \theta} + \overline{M}^{\psi}_{\theta x} \right\} dx \Big|_{\theta=0,\theta_0} = 0 \tag{48}$$

$$\text{or} \qquad \delta\psi_x\big|_{\theta=0,\theta_0} = 0$$

$$\int_x \left\{ d^{2}_{6}\frac{\partial \psi_x}{\partial \theta^2} + d^{2}_{7}\frac{\partial^2 \psi_\theta}{\partial \theta \partial x} + \hat{R}^{h}_{\theta} \right\} dx \Big|_{\theta=0,\theta_0} = 0 \qquad \text{or} \qquad \delta\left(\frac{\partial \psi_x}{\partial \theta}\right)\Big|_{\theta=0,\theta_0} = 0 \tag{49}$$

$$\int_x \left\{ e^{2}_{1}\frac{\partial V}{\partial \theta} + e^{2}_{2}\frac{\partial^2 W}{\partial x^2} + e^{2}_{3}\frac{\partial^2 W}{\partial \theta^2} + e^{2}_{4}\frac{\partial \psi_x}{\partial x} + e^{2}_{5}\frac{\partial^3 \psi_x}{\partial x\,\partial \theta^2} + e^{2}_{6}\frac{\partial \psi_\theta}{\partial \theta} + e^{2}_{7}\frac{\partial^3 \psi_\theta}{\partial x^2 \partial \theta} + \overline{M}^{\psi}_{\theta\theta} \right\} dx \Big|_{\theta=0,\theta_0} = 0 \qquad \text{or} \qquad \delta\psi_\theta\big|_{\theta=0,\theta_0} = 0 \tag{50}$$

$$\int_x \left\{ f^{2}_{1}\frac{\partial \Phi}{\partial \theta} + f^{2}_{2}\frac{\partial^2 V}{\partial x^2} + f^{2}_{3}\frac{\partial W}{\partial \theta} + f^{2}_{4}\frac{\partial^2 U}{\partial \theta \partial x} + f^{2}_{5} V + f^{2}_{6}\psi_\theta \right\} dx \Big|_{\theta=0,\theta_0} = 0 \tag{51}$$

$$\text{or} \qquad \delta\Phi\big|_{\theta=0,\theta_0} = 0$$

The constant coefficients $a^1_1 - a^1_8$, $b^1_1 - b^1_{15}$, $c^1_1 - c^1_{14}$, $d^1_1 - d^1_5$, $e^1_1 - e^1_7$, $f^1_1 - f^1_5$ and $a^2_1 - a^2_{14}$, $b^2_1 - b^2_{11}$, $c^2_1 - c^2_{16}$, $d^2_1 - d^2_7$, $e^2_1 - e^2_7$, $f^2_1 - f^2_6$ of Eqs. (29)-(46) are presented in Appendix B.

Relations presented in Eqs. (28)-(33) are equations of motion of a cylindrical shell with account deformation and rotary inertia according electromecanical consistent couple-stress theory in general form. Eqs. (34)-(51) are classical and non-classical boundaries conditions in general form.

3.1 Analysis of free vibrations of simple-simple nanoshell

In this section, a simple-simple supported cylindrical shell is investigated and its equations are developed. Since in simple-simple cylindrical nanoshells the boundary conditions are applied to the two ends of the nanoshell, therefore, because of the invariability of θ, the boundary conditions in Eqs. (43)-(51) already exist but boundary conditions in Eqs. (34)-(42) remain to be satisfied. In view of the boundary conditions in Eqs. (34)-(42), the geometric boundary conditions in Eqs. (35) and (37) are in this fashion

$$V = W = \Phi\big|_{x=0,L} = 0 \tag{52}$$

Besides, because the two ends are free from bending moments and higher order stresses in the classic case, other natural boundary conditions in Eqs. (34)-(42) are simplified as follows

$$\left(a^{1}_{1}\frac{\partial U}{\partial x} + a^{1}_{2}\frac{\partial^3 U}{\partial x\,\partial \theta^2} + a^{1}_{3}\frac{\partial^3 V}{\partial x^2 \partial \theta} + a^{1}_{4}\frac{\partial V}{\partial \theta} + a^{1}_{5} W + a^{1}_{6}\frac{\partial^2 W}{\partial \theta^2} + a^{1}_{7}\frac{\partial \psi_\theta}{\partial \theta} \right. \tag{53}$$

$$+a_8^1\frac{\partial^2\Phi}{\partial\theta^2}\Bigg)\Bigg|_{x=0,\mathrm{L}}=0 \tag{53}$$

$$\left(b_{10}^1\frac{\partial^2 V}{\partial x^2}+b_{11}^1 V+b_{12}^1\frac{\partial^2 U}{\partial x\,\partial\theta}+b_{13}^1\frac{\partial W}{\partial\theta}+b_{14}^1\psi_\theta+b_{15}^1\frac{\partial\Phi}{\partial\theta}\right)\Bigg|_{x=0,L}=0 \tag{54}$$

$$\left(c_{10}^1\frac{\partial^2 W}{\partial x^2}+c_{11}^1\frac{\partial^2 W}{\partial\theta^2}+c_{12}^1\frac{\partial\psi_\theta}{\partial\theta}+c_{13}^1\frac{\partial\psi_x}{\partial x}+c_{14}^1\frac{\partial V}{\partial\theta}\right)\Bigg|_{x=0,L}=0 \tag{55}$$

$$\left(d^1{}_1\frac{\partial^2 W}{\partial x^2}+d^1{}_2\frac{\partial^2 W}{\partial\theta^2}+d^1{}_3\frac{\partial\psi_\theta}{\partial\theta}+d_4^1\frac{\partial\psi_x}{\partial x}+d^1{}_5\frac{\partial V}{\partial\theta}+d^1{}_6\frac{\partial^3\psi_\theta}{\partial\theta\partial x^2}+d^1{}_7\frac{\partial^3\psi_x}{\partial\theta^2\partial x}\right)\Bigg|_{x=0,L}=0 \tag{56}$$

$$\delta\psi_\theta\big|_{x=0,L}=0 \tag{57}$$

$$\left(e_7^1\frac{\partial^2\psi_x}{\partial x\,\partial\theta}+e_8^1\frac{\partial^2\psi_\theta}{\partial x^2}\right)_{x=0,L}=0 \tag{58}$$

Eqs. (28)-(33) and boundary conditions in Eqs. (53)-(58) are considered the governing equations of motion of a simple-simple supported piezoelectric cylindrical nanoshell based on the Hajesfandiary's consistent theory and first order shear deformation theory. In these equations, if l = 0, the governing equations are reduced to shell equations of the first order shear theory in the classical continuum theory.

3.2 Analysis of free vibrations of clamped-clamped nanoshell

The following conditions hold at the two ends of a clamped-clamped supported cylindrical nanoshell

$$u=v=w=\psi_x=\psi_\theta=\Phi\big|_{x=0,L}=0 \tag{59}$$

Eq. (59) demonstrates that deformation and slope are zero at the two ends of the clamped-clamped supported nanotube

Therefore, boundary conditions in Eqs. (34), (35), (37), (38), (39) and (42) are in place. Hence, boundary conditions in Eqs. (38), (36) and (41) must be satisfied.

Because the two ends are free from bending moments in the classical case and higher order stresses in the nonclasscial case, these conditions are simplified as follows

$$\int_\theta\left\{b_{10}^1\frac{\partial^2 V}{\partial x^2}+b_{11}^1 V+b_{12}^1\frac{\partial^2 U}{\partial x\,\partial\theta}+b_{13}^1\frac{\partial W}{\partial\theta}+b_{14}^1\psi_\theta+b_{15}^1\frac{\partial\Phi}{\partial\theta}\right\}d\theta\Bigg|_{x=0,L}=0 \tag{60}$$

$$\int_\theta\left\{c_{10}^1\frac{\partial^2 W}{\partial x^2}+c_{11}^1\frac{\partial^2 W}{\partial\theta^2}+c_{12}^1\frac{\partial\psi_\theta}{\partial\theta}+c_{13}^1\frac{\partial\psi_x}{\partial x}+c_{14}^1\frac{\partial V}{\partial\theta}\right\}d\theta\Bigg|_{x=0,L}=0 \tag{61}$$

$$\int_{\theta}\left\{e_7^1\frac{\partial^2\psi_x}{\partial x\,\partial\theta}+e_8^1\frac{\partial^2\psi_\theta}{\partial x^2}\right\}d\theta\Bigg|_{x=0,L}=0 \tag{62}$$

4. Solution methods

In order to analyze the vibrations of the short piezoelectric cylindrical nanoshell and investigate the parameters affecting the vibration frequencies of the system, the governing equations and boundary conditions must be solved. In this paper, two simple-simple and clamped-clamped support cases on the two edges of the nanotube are solved. The first case, simply-supported edges, is solved using Navier solution and the second case, clamped-clamped edges, is solved using EKM. Besides, system frequencies are investigated for different parameters. Moreover, the validity of the results obtained using the Navier solution for the clamped-clamped piezoelectric nanoshell is compared with those obtained using the EKM, and the results are reported in the literature.

4.1 Navier solution method

In order to solve the governing equations together related boundaries conditions, since the nano-shell has simply supported, the Navier procedure is used by assuming the displacement field as follows (Leissa 1993)

$$\begin{aligned}
U(x,\theta,t)&=\sum_n\sum_m U_0e^{I\omega t}\cos(\frac{m\pi x}{L})\ \cos(n\theta)\\
V(x,\theta,t)&=\sum_n\sum_m V_0e^{I\omega t}\sin(\frac{m\pi x}{L})\ \sin(n\theta)\\
W(x,\theta,t)&=\sum_n\sum_m W_0e^{I\omega t}\sin(\frac{m\pi x}{L})\ \cos(n\theta)\\
\psi_x(x,\theta,t)&=\sum_n\sum_m \psi_{x0}e^{I\omega t}\cos(\frac{m\pi x}{L})\ \cos(n\theta)\\
\psi_\theta(x,\theta,t)&=\sum_n\sum_m \psi_{\theta0}e^{I\omega t}\sin(\frac{m\pi x}{L})\ \sin(n\theta)\\
\Phi(x,\theta,t)&=\sum_n\sum_m \phi e^{I\omega t}\sin(\frac{m\pi x}{L})\ \cos(n\theta)
\end{aligned} \tag{63}$$

where *m* and *n* are the axial and circumferential half-wave numbers, respectively.

According to the above equation can be seen that essential boundary conditions in Eq. (52) and natural boundary conditions in Eqs. (53)-(58) are satisfied.

By substituting Eq. (63) in Eqs. (28)-(33), the final equations are rewritten in a matrix form as follows

$$[k]\{d\}+[M]\{\ddot{d}\}=0 \tag{64}$$

So the results are written as follows (Zeighampour and Tadi Beni 2014)

$$([K]+\omega^2[M])\{d_0\}=0 \tag{65}$$

where $\{d_0\}^T = \{U_0 V_0 W_0 \psi_x \psi_\theta \phi\}^T$ is the undetermined displacement amplitude vector and ω is the frequency. To obtain a non-trivial solution of Eq. (65), it is necessary to set the determinant of the coefficient matrix to zero.

4.2 Extended Kantorovich method

The extended Kantorovich method is one of the weighted residual methods used to solve differential equations. Being free from limitations in the support conditions of shells, and enjoying high precisions and acceptable speed. This method is one of the appropriate methods for analyzing the bending of plates and shells, an area which recently has appealed to researchers. This method is based on converting partial differential equations (PDEs) governing the deformation of plates and shells into a set of ordinary differential equations (ODEs) by considering the deformation function as two independent functions. The most shape investigated in this method had rectangular, circular, cylindrical shapes and were mostly under clamped support condition. The extended Kantorovich solution is a method with high convergence speed in which convergence is achieved after three to four iterations. This method was initially used by Kerr (1968) in the semi-analytic solution of two-dimensional problems of sold mechanics. Today, this method is extensively used to solve solid mechanics problems including eigenvalue, buckling, bending and vibration of plates and shells.

In this method, the two-variable function is converted to the multiplication product of two functions as follows

$$f(x,\theta) = f_1(x) \times g_1(\theta) \tag{66}$$

According to this definition, the displacement and rotation functions of the problem are written as

$$\mathrm{u}(x,\theta) = f_1(x) \times g_1(\theta) \tag{67}$$

$$\mathrm{v}(x,\theta) = f_2(x) \times g_2(\theta) \tag{68}$$

$$\mathrm{w}(x,\theta) = f_3(x) \times g_3(\theta) \tag{69}$$

$$\psi_x(x,\theta) = f_4(x) \times g_4(\theta) \tag{70}$$

$$\psi_\theta(x,\theta) = f_5(x) \times g_5(\theta) \tag{71}$$

$$\Phi(x,\theta) = f_6(x) \times g_6(\theta) \tag{72}$$

The initial functions g_i for $i = 1...6$ are assumed as follows

$$g_1 = \left(\cosh(\frac{\tau.\theta}{2\pi}) - \cos(\frac{\tau.\theta}{2\pi}) - \left(\frac{\cosh(\tau)-\cos(\tau)}{\sinh(\tau)-\sin(\tau)}\right)\right).\left(\sinh(\frac{\tau.\theta}{2\pi}) - \sin(\frac{\tau.\theta}{2\pi})\right) \tag{73}$$

$$\mathrm{g}_2 = 1 - \cos(2\pi\theta) \tag{74}$$

$$g_3 = \left(\cosh(\frac{\tau.\theta}{2\pi}) - \cos(\frac{\tau.\theta}{2\pi}) - \left(\frac{\cosh(\tau) - \cos(\tau)}{\sinh(\tau) - \sin(\tau)} \right) \right) . \left(\sinh(\frac{\tau.\theta}{2\pi}) - \sin(\frac{\tau.\theta}{2\pi}) \right) \tag{75}$$

$$g_4 = \left(\cosh(\frac{\tau.\theta}{2\pi}) - \cos(\frac{\tau.\theta}{2\pi}) - \left(\frac{\cosh(\tau) - \cos(\tau)}{\sinh(\tau) - \sin(\tau)} \right) \right) . \left(\sinh(\frac{\tau.\theta}{2\pi}) - \sin(\frac{\tau.\theta}{2\pi}) \right) \tag{76}$$

$$g_5 = \theta.(\theta - 2\pi) \tag{77}$$

$$g_6 = \theta.(\theta - 2\pi) \tag{78}$$

The value τ =4.7030040745 is taken into consideration. By substituting these initial functions into Eqs. (67)-(72), considering the solution method based on weighted residual, each of the equilibrium equations in the interval θ = 0 – 2 π is integrated in relation to5.Therefore, partial differential equations turn into ordinary differential equations, and these equations are merely a function of f_i's i = 1 .... 6 based on Eqs. (79)-(84).

$$\begin{aligned} eq_1 = {} & a_1 \frac{d^2}{dx^2} f_1(x) + a_2 \frac{d^2}{dx^2} f_1(x) + a_3 f_1(x) + a_4 f_1(x) + a_5 \frac{d^3}{dx^3} f_2(x) \\ & + a_6 \frac{d}{dx} f_2(x) + a_7 \frac{d^3}{dx^3} f_1(x) + a_8 \frac{d}{dx} f_3(x) + a_9 \frac{d}{dx} f_3(x) + a_1 \frac{d}{dx} f_{05}(x) \\ & + a_{11} f_4(x) - a_{12}.\omega^2 f_1(x) = 0 \end{aligned} \tag{79}$$

$$\begin{aligned} eq_2 = {} & b_1 \frac{d^4}{dx^4} f_2(x) + b_2 \frac{d^2}{dx^2} f_2(x) + b_3 f_2(x) + b_4 \frac{d^2}{dx^2} f_2(x) + b_5 f_2(x) \\ & + b_6 \frac{d^3}{dx^3} f_1(x) + a_7 \frac{d}{dx} f_1(x) + b_8 \frac{d}{dx} f_1(x) + b_9 \frac{d^2}{dx^2} f_3(x) + b_{10} f_3(x) + b_{11} f_3(x) \\ & + b_{12} \frac{d}{dx} f_4(x) + b_{13} f_5(x) b_{14} f_5(x) + b_{15} \frac{d^2}{dx^2} f_5(x) + b_{16} f_6(x) - b_{17}.\omega^2 f_2(x) = 0 \end{aligned} \tag{80}$$

$$\begin{aligned} eq_3 = {} & c_1 \frac{d^4}{dx^4} f_3(x) + c_2 \frac{d^2}{dx^2} f_3(x) + c_3 \frac{d^2}{dx^2} f_3(x) + c_4 f_3(x) + c_5 f_3(x) + c_6 f_3(x) \\ & + c_7 \frac{d}{dx} f_1(x) + c_8 \frac{d}{dx} f_1(x) + c_9 \frac{d^2}{dx^2} f_2(x) + c_1 f_2(x) + c_1 f_2(x) + c_1 \frac{d}{dx} f_4(x) \\ & + c_{13} \frac{d^3}{dx^3} f_4(x) + c_{14} \frac{d}{dx} f_4(x) + c_{15} f_5(x) + c_{16} f_5(x) + c_{17} \frac{d^2}{dx^2} f_5(x) \\ & + c_{18} \frac{d^2}{dx^2} f_6(x) + c_{19} f_6(x) - c_{20}.\omega^2 f_3(x) = 0 \end{aligned} \tag{81}$$

$$eq_4 = d_1 \frac{d^2}{dx^2} f_4(x) + d_2 \frac{d^2}{dx^2} f_4(x) + d_3 f_4(x) + d_4 f_4(x) + d_5 f_4(x) \tag{82}$$

$$+d_6\frac{d}{dx}f_5(x)+d_7\frac{d}{dx}f_5(x)+d_8\frac{d^3}{dx^3}f_5(x)+d_9f_1(x)+d_{10}\frac{d}{dx}f_2(x)$$
$$+d_{11}\frac{d^3}{dx^3}f_3(x)+d_{12}\frac{d}{dx}f_3(x)+d_{13}\frac{d}{dx}f_3(x)+d_{14}\frac{d}{dx}f_6(x)+d_{15}.\omega^2f_4(x)=0 \tag{82}$$

$$eq_5=e_1\frac{d^4}{dx^4}f_5(x)+e_2\frac{d^2}{dx^2}f_5(x)+e_3\frac{d^2}{dx^2}f_5(x)+e_4f_5(x)+e_5f_5(x)$$
$$+e_6\frac{d}{dx}f_4(x)+e_7\frac{d}{dx}f_4(x)+e_8\frac{d^3}{dx^3}f_4(x)+e_9\frac{d}{dx}f_1(x)+e_{10}\frac{d^2}{dx^2}f_2(x)$$
$$+e_{11}f_2(x)+e_{12}f_2(x)+e_{13}\frac{d^2}{dx^2}f_3(x)+e_{14}f_3(x)+e_{15}f_3(x)+e_{16}f_6(x)$$
$$-e_{17}.\omega^2f_5(x)=0 \tag{83}$$

$$eq_6=f_1\frac{d^2}{dx^2}f_6(x)+f_2f_6(x)+f_3f_6(x)+f_4f_2(x)+f_5\frac{d}{dx}f_4(x)+f_6f_5(x)$$
$$+f_7\frac{d^2}{dx^2}f_5(x)+f_8f_3(x)=0 \tag{84}$$

The constants of the foregoing equations are determined by integrating g_i functions in relation to θ in $\theta = 0 - 2\pi$ interval based on programing.

Afterwards, by solving the ordinary differential equation system and by considering the boundary conditions according to Eq. (59) for the clamped-clamped support and for the simple-simple support according to Eq. (52) the f_i functions are developed. The boundary conditions applied in the discretization method are defined based on Eqs. (85) and (86) for the cylindrical shell with clamped-clamped boundary conditions, and based on Eqs. (87) and (88) for the simple-simple boundary conditions.

$$\mathrm{f}_i=0,\mathrm{i}=1...6 \qquad x=0,L \tag{85}$$

$$g_i=0,\mathrm{i}=1...6 \qquad \theta=0,2\pi \tag{86}$$

$$f_2=f_3=f_5=0 \qquad x=0,L \tag{87}$$

$$g_1=g_3=g_4=0 \qquad \theta=0,2\pi \tag{88}$$

After determining f_i functions by solving the Eqs. (79)-(84) and substituting them into equilibrium equations, these stages are iterated and the ordinary differential equations based on θ are determined according to Eqs. (89)-(94).

$$eq_1=k_1h_1(\theta)+k_2\frac{d^2}{d\theta^2}h_1(\theta)+k_3\frac{d^2}{d\theta^2}h_1(\theta)+k_4\frac{d^4}{d\theta^4}h_1(\theta)+k_5\frac{d}{d\theta}h_2(\theta) \tag{89}$$

$$+k_6\frac{d}{d\theta}h_2(\theta)+k_7\frac{d^3}{d\theta^3}h_2(\theta)+k_8h_3(\theta)+k_9\frac{d^2}{d\theta^2}h_3(\theta)+k_{10}\frac{d}{d\theta}h_5(\theta)$$
$$+k_{11}\frac{d^2}{d\theta^2}h_4(\theta)-k_{12}.\omega^2h_1(\theta)=0 \tag{89}$$

$$eq_2=l_1h_2(\theta)+l_2h_2(\theta)+l_3\frac{d^2}{d\theta^2}h_2(\theta)+l_4\frac{d^2}{d\theta^2}h_2(\theta)+l_5h_2(\theta)+l_6\frac{d}{d\theta}h_1(\theta)$$
$$+l_7\frac{d^3}{d\theta^3}h_1(\theta)+l_8\frac{d}{d\theta}h_1(\theta)+l_9\frac{d}{d\theta}h_3(\theta)+l_{10}\frac{d^3}{d\theta^3}h_3(\theta)+l_{11}\frac{d}{d\theta}h_3(\theta)$$
$$+l_{12}\frac{d}{d\theta}h_4(\theta)+l_{13}\frac{d^2}{d\theta^2}h_5(\theta)+l_{14}h_5(\theta)+l_{15}h_5(\theta)+l_{16}\frac{d}{d\theta}h_6(\theta)$$
$$-l_{17}.\omega^2h_2(\theta)=0 \tag{90}$$

$$eq_3=o_1h_3(\theta)+o_2h_3(\theta)+o_3\frac{d^2}{d\theta^2}h_3(\theta)+o_4\frac{d^4}{d\theta^4}h_3(\theta)+o_5\frac{d^2}{d\theta^2}h_3(\theta)+o_6h_3(\theta)$$
$$+o_7h_1(\theta)+o_8\frac{d^2}{d\theta^2}h_1(\theta)+o_9\frac{d}{d\theta}h_2(\theta)+o_1\ \frac{d}{d\theta}h_{20}(\theta)+o_1\ \frac{d^3}{d\theta^3}h_{12}(\theta)$$
$$+o_{12}\frac{d^2}{d\theta^2}h_4(\theta)+o_{13}h_4(\theta)+o_{14}h_4(\theta)+o_{15}\frac{d^3}{d\theta^3}h_5(\theta)+o_{16}\frac{d}{d\theta}h_5(\theta)+o_{17}\frac{d}{d\theta}h_5(\theta)$$
$$+o_{18}h_6(\theta)+o_{19}\frac{d^2}{d\theta^2}h_6(\theta)-o_{20}.\omega^2h_3(\theta)=0 \tag{91}$$

$$eq_4=p_1h_4(\theta)+p_2\frac{d^2}{d\theta^2}h_4(\theta)+p_3\frac{d^4}{d\theta^4}h_4(\theta)+p_4\frac{d^2}{d\theta^2}h_4(\theta)+p_5h_4(\theta)$$
$$+p_6\frac{d}{d\theta}h_5(\theta)+p_7\frac{d^3}{d\theta^3}h_5(\theta)+p_8\frac{d}{d\theta}h_5(\theta)+p_9\frac{d^2}{d\theta^2}h_1(\theta)+p_{10}\frac{d}{d\theta}h_2(\theta)$$
$$+p_{11}h_3(\theta)+p_{12}\frac{d^2}{d\theta^2}h_3(\theta)+p_{13}h_3(\theta)+p_{14}h_6(\theta)-\mathrm{p}_{15}.\omega^2h_4(\theta)=0 \tag{92}$$

$$eq_5=q_1h_5(\theta)+q_2h_5(\theta)+q_3\frac{d^2}{d\theta^2}h_5(\theta)+q_4\frac{d^2}{d\theta^2}h_5(\theta)+q_5h_5(\theta)+q_6\frac{d}{d\theta}h_4(\theta)$$
$$+q_7\frac{d^3}{d\theta^3}h_4(\theta)+q_8\frac{d}{d\theta}h_4(\theta)+q_9\frac{d}{d\theta}h_1(\theta)+q_{10}h_2(\theta)+q_{11}\frac{d^2}{d\theta^2}h_2(\theta)$$
$$+q_{12}h_2(\theta)+q_{13}\frac{d}{d\theta}h_3(\theta)+q_{14}\frac{d^3}{d\theta^3}h_3(\theta)+q_{15}\frac{d}{d\theta}h_3(\theta)+q_{16}\frac{d}{d\theta}h_6(\theta)$$
$$-q_{17}.\omega^2h_5(\theta)=0 \tag{93}$$

$$eq_6=r_1h_6(\theta)+q+r_2\frac{d^2}{d\theta^2}h_6(\theta)+r_3h_6(\theta)+r_4\frac{d}{d\theta}h_2(\theta)+\mathrm{r}_5\,h_4(\theta)+r_6\frac{d}{d\theta}h_5(\theta) \tag{94}$$

$$+r_7 h_3(\theta) + r_8 \frac{d^2}{d\theta^2} h_3(\theta) = 0 \tag{94}$$

The constants of the foregoing equations are developed by integrating the f_i functions determined by solving differential equations in the preceding section in relation to x in $x = 0 - L$interval according to programing in the software program. Here, too, by solving differential equation system, the g_i functions are computed and the first iteration cycle ends. The main advantage of the extended Kantorovich solution is its high convergence speed. In this method, by solving different problems, only after 3 to 4 iterations, an acceptable solution is achieved, and, consequently, the vibrational frequencies are determined.

5. Results and discussions

In this section, the vibrational results of the piezoelectric cylindrical nanoshell under simple-simple and clamped-clamped support conditions are presented. The nanoshell is assumed to be made of BaTiO3 and the material properties of which are presented in Table 1. To analyze the vibration, the cylindrical nanoshell is assumed to be short, with a thickness of h = 1 nm and a radius-thickness ratio of $\frac{R}{h} = 10$. Since the nanoshell is assumed to be short, the length-radius ratio is $\frac{L}{R} = 1$.

Since there are no available empirical or molecular dynamics results for the size effect parameter of the present theory for cylindrical nanoshells, the dimensionless parameter $\left(\frac{l}{h}\right)$ was used in different numerical cases to analyze the size effect of the short piezoelectric cylindrical nanoshell.

5.1 Validation of results

Before addressing the vibrational analysis of the piezoelectric cylindrical nanoshell, using Ke *et al*. (2014b)'s differential quadrature (DQ) solution and Markus' precise solution (1988) for a cylindrical nanoshell with h = 1 nm made of PZT-4 material the characteristics of which are presented in Table 1, and by ignoring the piezoelectric effect and size effect for m = 1, the results presented in Table 2 demonstrate good consistency between the results of the present study and the results of previous studies in this context.

Table 1 PZT-4 material properties

Properties	PZT-4
Young's module(GPa)	790
Possion's coefficient	0.3
mass density(Kg.m^{-3})	6500

Table 2 Comparison of dimensionless natural frequency $\left(\Omega R\sqrt{\frac{(1-\nu^2)\rho}{E}}\right)$ for S-S cylindrical shell with h = 1 nm, $\frac{L}{R}=20$, $\frac{h}{R}=0.05$, ν = 0.3, m = 1

n	Present model	Markus (1988)	Ke *et al*. (2014a, b)
1	0.016211	0.016106	0.016112
2	0.039647	0.039233	0.039352
3	0.109783	0.10948	0.109863
4	0.209182	0.20901	0.210317

Table 3 Comparison of dimensionless natural frequency $\left(\Omega R\sqrt{\frac{(1-\nu^2)\rho}{E}}\right)$ for S-S and C-C cylindrical shell with h = 1 nm, $\frac{L}{R}=20$, $\frac{h}{R}=0.01$, ν = 0.3, m = 1

n	S-S			C-C		
	Present model	Ke *et al*. (2014b)	Loy *et al*. (1997)	Present model	Ke *et al*. (2014b)	Loy *et al*. (1997)
1	0.016106	0.01608	0.016101	0.032793	0.032760	0.032885
2	0.009451	0.009381	0.009382	0.013958	0.013893	0.013932
3	0.022179	0.022109	0.022105	0.022755	0.022671	0.022672
4	0.042159	0.042099	0.042095	0.042285	0.042213	0.042208

Table 4 BaTiO3 material properties

Properties	BaTiO3
Young's module (GPa)	113.7
Mass density (Kg.m^{-3})	6020
Flexoelectric effect (μc.m^{-1})	10-15
Permitivity effect ($s^2 \cdot c^2$/kg.m^3)	1.239
Possion's coefficient	0.325

Besides, by ignoring the piezoelectric effect and size effect, another comparison has been drawn using the analysis of nonlocal vibrations by Ke *et al*. (2014b) using Loy *et al*. (1997)'s DQ method for a nanoshell made of PZT-4 with the physical characteristics h = 1 nm, $\frac{L}{R}=20$, $\frac{h}{R}=0.01$, ν = 0.3, m = 1. The results of the comparison are demonstrated in Table 3.

As can be seen, in this validation, too, the results achieved for the simple-simple support conditions using the Navier solution and for the clamped-clamped support condition using extended Kantorovich method are consistent with other studies conducted in this context.

5.2 Effect of various parameter on electromechanical free vibrations of nanoshell

Table 5 is a numerical demonstration presenting the effect of material length parameter $\left(\frac{l}{h}\right)$ on the dimensionless frequency $\Omega R\sqrt{\frac{(1-\nu^2)\rho}{E}}$ of simple-simple cylindrical nanoshell for different half-wave numbers n and for $m = 1$. By setting the size parameter to zero in this theory, the classical theory is developed. In the light of the results, increase in the size parameter leads to increase in the natural frequency of piezoelectric nanoshell. This increase is due to increased rigidity accompanied by increased size effect parameter. This demonstrates the dependency of nanoshell vibration on the mechanical size of the nanoshell in the nanoscale, and, therefore, the classical theory is unable to predict the precise behavior of mechanical systems in the nanoscale. Besides, the effect of size parameter in higher half-wave numbers is more considerable than its effect in lower half-wavenumbers. With the increase in the number of half-wave n, first the natural frequencies decrease and then they increase.

Table 5 The effect of size effect parameter $\left(\frac{l}{h}\right)$ on dimensionless natural frequency for different circumferential wavenumbers

n	$l = 0$	$l = h$	$l = 2h$	$l = 3h$	$l = 4h$
1	2.048386	2.081868	2.174969	2.309658	2.465892
2	1.987116	2.072112	2.23221	2.386229	2.547951
3	0.72322	1.252881	1.957413	2.458328	2.831793
4	1.205462	1.751557	2.53314	3.125343	3.594929
5	2.511313	2.861201	3.488144	4.090461	4.600823
6	3.673388	3.929144	4.518465	5.188888	5.69501
7	4.521215	4.820628	5.570554	6.357348	6.796686
8	5.185088	5.616799	6.663762	7.543406	7.88377
9	5.800003	6.401867	7.821266	8.705466	8.960536
10	6.402419	7.208209	9.052431	9.836556	10.0329

Table 6 Comparison of numerical result between Navier and EK methods for S-S condition

l/h	Navier method	EK method
0	1.93757	1.89235
0.5	1.96900	1.91713
1	2.05611	1.98784
1.5	2.18172	2.09736
2	2.32691	2.23609
2.5	2.47623	2.39440
3	2.61802	2.56403

The lowest amount of frequency takes place in $n = 2 – 3$, which indicates that for a nanoshell with $h = 1$ nm, $\frac{L}{R} = 1$, $\frac{R}{h} = 20$, $m = 1$ characteristics, the main frequency of free vibration is in the half-wave $n = 2 – 3$.

Table 6 draws a comparison between Navier and extended Kantorovich methods. The results have been achieved for a simple-simple supported piezoelectric nanoshell with two solutions. As can be seen, the results have high consistency despite a minute difference.

Figs. 2 and 3 demonstrate the effect of material length scale parameter on dimensionless frequency $\left(\Omega R\sqrt{\frac{(1-\nu^2)\rho}{E}}\right)$ in the two cases of the current and classical theories for the two

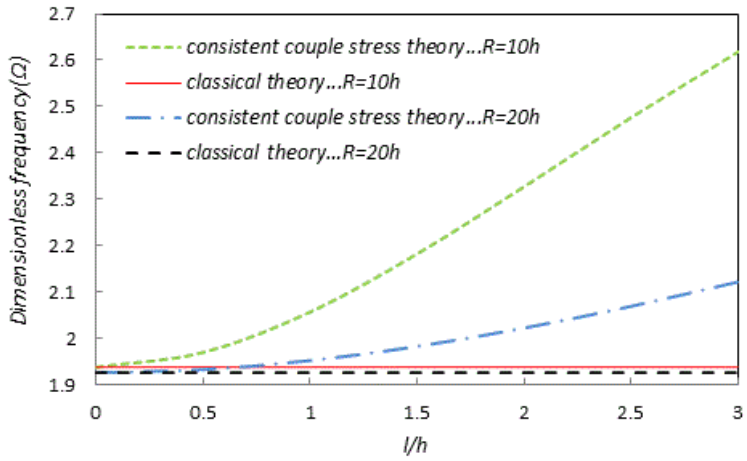

Fig. 2 Effect of material length scale parameter on dimensionless natural frequency for S-S, in different theory, $m = 1$

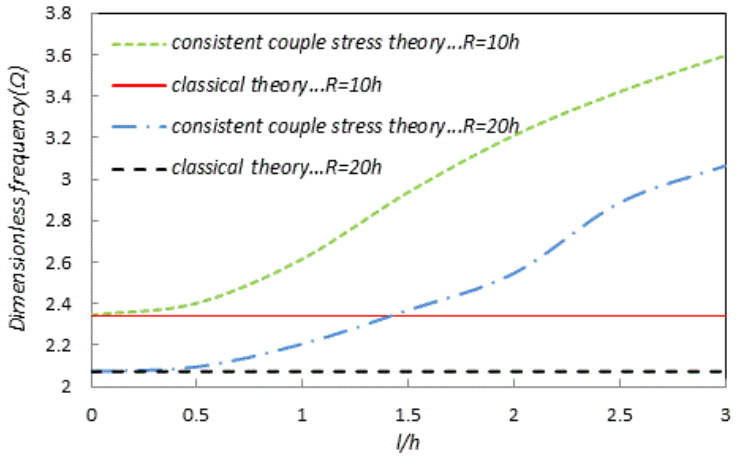

Fig. 3 Effect of material length scale parameter on dimensionless natural frequency for C-C, in different theory, $m = 1$

simply supported and clamped supported cases for half-wave number m = 1. As illustrated by the diagrams, in the present theory, the vibration frequency in the nanoscale is completely dependent on the mechanical size and demonstrates more precise numerical results in comparison with the classical theory. In fact, the use of classical theories to investigate the vibrational behavior of nanotubes and their size dependency does not yield precise results. The figures clearly demonstrate the increase in nanoshell natural frequency as a result of increased size effect. This increase is due to increased nanotube rigidity in higher values of size effect parameter in the couple stress theory.

Figs. 4 and 5 demonstrate the effect of coefficient of nanoshell radius-thickness ratio $\left(\frac{R}{h}\right)$ on frequency for different size effect values in simply and clamped supported conditions. Since in higher $\left(\frac{R}{h}\right)$ the nanoshell indeed becomes thinner and hence its stiffness reduces, the vibrational frequency, too, is reduced as a result. As can be seen, the highest frequencies are related to clamped supports and lowest frequencies are related to simple supports. That is because clamped supports are the strongest in terms of stiffness and simple supports are the weakest. Besides, according to previous studies conducted on nanotube vibration, the nanotube is assumed thin in the $10 \le \frac{R}{h} \le 100$ interval and thick for $\left(\frac{R}{h}\right)$ ratios below 10. In this study, due to the assumption of thick nanoshell and consideration of shear stresses, the $\left(\frac{R}{h}\right) = 10$ coefficient is taken into account in all the results. As illustrated by Figs. 6 and 7, increase in the length-radius ratio $\left(\frac{L}{R}\right)$ of piezoelectric nanoshell and increase in nanotube length lead to increase in system stability and, as a result, decrease in vibrational frequencies which reach a stable and very low amount in very long lengths. Increase in nanotube length and decrease in system stiffness is accompanied by decrease in shell deformations and, as a result, decrease in vibration frequency.

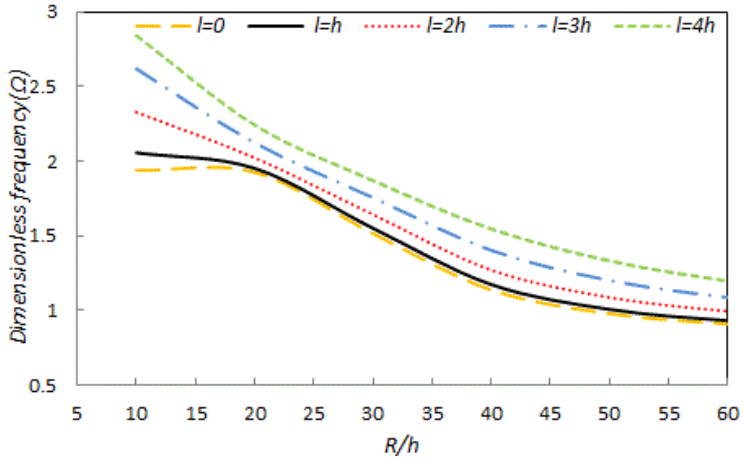

Fig. 4 The effect of the radius-to-thickness on the dimensionless natural frequency of piezoelectric cylindrical nanoshell for S-S

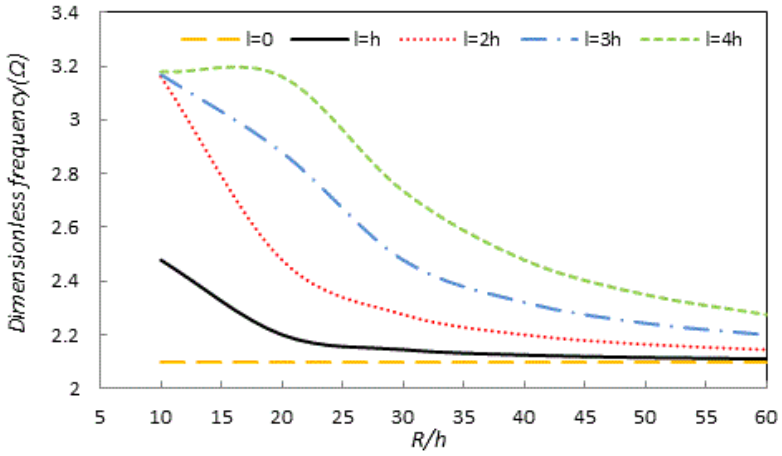

Fig. 5 The effect of the radius-to-thickness on the dimensionless natural frequency of piezoelectric cylindrical nanoshell for C-C

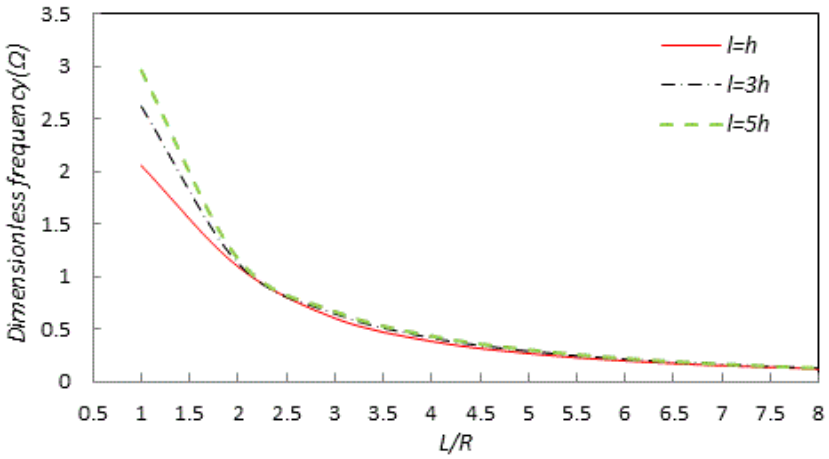

Fig. 6 The effect of the length-to-radius on the dimensionless natural frequency of piezoelectric cylindrical nanoshell for S-S

The flexoelectric effect of piezoelectric material on the vibrational frequency of piezoelectric nanoshell for a simple- simple case is demonstrated in Fig. 8. In this case, as Table 7 shows, the effect of flexoelectric coefficient in higher $\left(\frac{R}{h}\right)$'s is more than lower radius- thickness ratios. Also it should be noted that, in classic theory the changes of frequency resulting from a change of flexoelectric coefficient is very low, because according the consistent theory, the strong effect of flexoelectric appears in the strain gradient terms which deleted in the classical theory. In figure 8 the parameter α is defined as $\alpha = \frac{\omega - \omega_C}{\omega_C} \times 100$ for $\left(\frac{R}{h}\right) = 50$. The effect of the flexoelectric coefficient on the first order frequency, based on this coefficient, is displayed in Fig. 8. ω is the

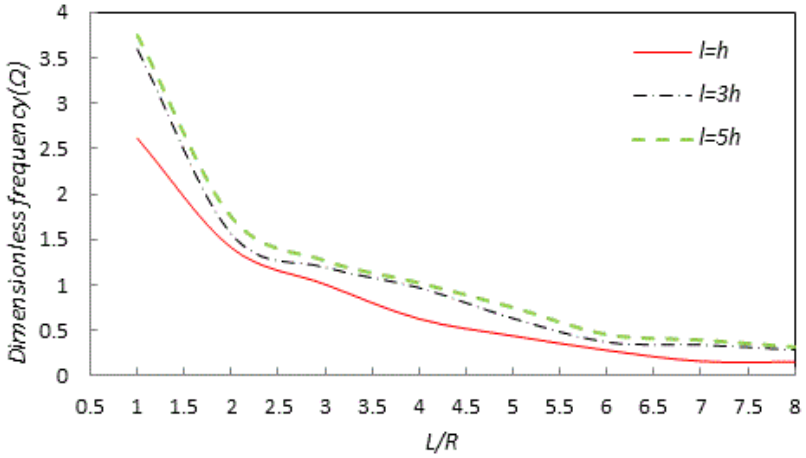

Fig. 7 The effect of the length-to-radius on the dimensionless natural frequency of piezoelectric cylindrical nanoshell for C-C

Table 7 The effect of flexoelectric coefficient on classic dimensionless natural frequency for different radius-thickness ratios $\left(\frac{R}{h}\right)$

Flexoelectric coefficient (μc/m)	R/h = 10	R/h = 20	R/h = 50
10	1.937575	1.925346	0.977846
11	1.937654	1.928584	1.003503
12	1.937713	1.930579	1.030489
13	1.937759	1.931915	1.058611
14	1.937795	1.932863	1.087685
15	1.937824	1.933565	1.117543

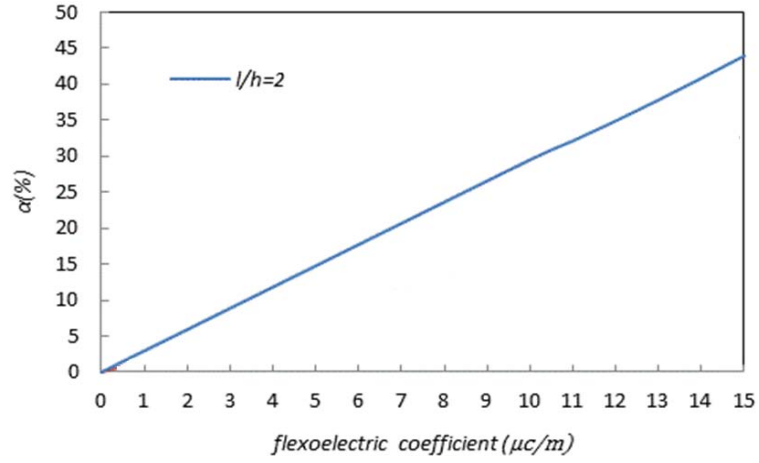

Fig. 8 The dimensionless relative frequency varying with flexoelectric coefficient

frequency for different flexoelectric coefficients $f = (10 - 15) \times 10^{-6}$ and ω_c is the frequency of nanoshell vibrations for $l = 0$. Fig. 8 demonstrates that increase in the flexoelectric coefficient of the material and, indeed, increase in the piezoelectric property of the material is accompanied by increase in natural frequency. However, since the amount of this increase is infinitesimal, the percentage equation $\alpha = \frac{\omega - \omega_C}{\omega_C} \times 100$ is used to show the effect of the flexoelectric coefficient on vibration frequency.

6. Conclusions

In this paper, considering the size effect on the short cylindrical shell and using first-order shear deformable model and the consistent couples stress theory, a new extended model was developed which incorporated equations of motion as well as classical and nonclassical boundary conditions. It should be noted that the new cylindrical thin shell model is reduced to the cylindrical thin shell in the consistent couple stress theory and the classical theory in special cases. This paper, the electromechanical vibrations of a short cylindrical nanotube made of piezoelectric material were investigated using Hadjesfandiari's consistent theory and first-order shear deformable theory. The new equations were developed using Hamilton's principle. Afterwards, for equations were solved using Navier and extended Kantorovich method for special cases of shells with simply-supported and clamped-supported. Afterwards, the validity of the results was examined using the results of other studies conducted in this context. The results had good consistency with previous studies. In those studies, the effects of various factors including material length scale parameter, length, thickness, half-wave numbers, and flexoelectric coefficient on the natural frequency of the system in the free vibration case had been investigated and analyzed.

- The diagrams demonstrate that increase in size parameter leads to increase in nanoshell stiffness and, consequently, increase in vibration frequency. These variations are more considerable in higher half-wave numbers.
- Moreover, considering the diagram of frequency variation in relation to $\left(\frac{L}{R}\right)$ and $\left(\frac{R}{h}\right)$, it is concluded that increase in the length or decrease in the diameter of nanotubes lead to increase in the frequency of vibrations.
- In all the diagrams, due to higher stiffness of clamped supports, the vibration frequency of clamped supports is higher than that of hinged-hinged supports.
- In addition, increase in flexoelectric coefficient strengthens the piezoelectric quality, and, therefore, leads to increased vibration frequency.
- The new equations developed by Hajefandiari's new theory and the results obtained by solving equations of motion and boundary conditions governing the vibrations of piezoelectric cylindrical nanotube can be used in future studies in the areas of buckling, vibration and pull-in, and in design and construction of advanced micro and nanoelectromechanical systems.

References

Akgoz, B. and Civalek, O. (2013), "Vibration analysis of micro-scaled sector shaped graphene surrounded

by an elastic matrix", *Computat. Mater. Sci.*, **77**, 295-303.
Akgoz, B. and Civalek, O. (2014), "A microstructure-dependent sinusoidal plate model based on the strain gradient elasticity theory", *Acta Mechanica*, **226**(7), 2277-2294.
Akgoz, B. and Civalek, O. (2015), "A novel microstructure-dependent shear deformable beam model", *Int. J. Mech. Sci.*, **99**, 10-20.
Asghari, M., Kahrobaiyan, M.H. and Ahmadian, M.T. (2010), "A nonlinear Timoshenko beam formulation based on the modified couple stress theory", *Int. J. Eng. Sci.*, **48**(12), 1749-1761.
Belkorissat, I., Sid, M., Houari, A., Tounsi, A., Adda Bedia, E.A. and Mahmoud, S.R. (2015), **"**On vibration properties of functionally graded nano-plate using a new nonlocal refined four variable mode", *Steel Compos. Struct., Int. J.*, **18**(4), 1063-1081.
Buhlmann, S., Dwir, B., Baborowski, J. and Muralt, P. (2002), "Size effects in mesoscopic epitaxial ferroelectric structures: Increase of piezoelectric response with decreasing feature-size", *Appl. Phys. Lett.*, **80**(17), 3195-3197.
Chakraverty, S. and Behera, L. (2015), "Small scale effect on the vibration of non-uniform nanoplates", *Struct. Eng. Mech., Int. J.*, **55**(3), 495-510.
Chen, C.Q., Shi, Y., Zhang, Y.S., Zhu, J. and Yan, Y.J. (2006), "Size dependence of Young's modulus in ZnO nanowires", *Phys. Rev. Lett.*, **96**(7), 075505.
Civalek, O. (2006), "The determination of frequencies of laminated conical shells via the discrete singular convolution method", *J. Mech. Mater. Struct.*, **1**(1), 163-182.
Civalek, O. and Gürses, M. (2009), "Free vibration analysis of rotating cylindrical shells using discrete singular convolution technique", *Int. J. Press. Vessels Pip.*, **86**(10), 677-683.
Cosserat, E. and Cosserat, F. (1909), *Théorie des corps de´formables [Theory of Deformable Bodies]*, A. Hermann et Fils, Paris, France.
Cross, L.E. (2006), "Flexoelectric effects: charge separation in insulating solids subjected to elastic strain gradients", *J. Mater. Sci.*, **41**(1), 53-63.
Ebrahimi, F. and Salari, E. (2016), "Thermal loading effects on electro-mechanical vibration behavior of piezoelectrically actuated inhomogeneous size-dependent Timoshenko nanobeams", *Adv. Nano Res., Int. J.*, **4**(3), 197-228.
Eliseev, E.A., Morozovska, A.N. and Glinchuk, M.D. (2009), "Pontaneous/flexoelectric/flexomagnetic effect in nanoferroics", *Phys. Rev. B: Condens Matter*, **79**(16), 165-433.
Eringen, A.C. (1983), "On differential equations of nonlocal elasticity and solutions of screw dislocation and surface waves", *J. Appl. Phys.*, **54**(9), 4703-4710.
Gao, Y. and Bando, Y. (2002), "Nanotechnology: Carbon nanothermometer containing gallium", *Nature*, **415**(6872), 599-600.
Ghorbanpour Arani, A., Shokravi, M. and Mozdianfard, M.R. (2012a), "Nonlocal electro-thermal transverse vibration of embedded fluid-conveying DWBNNTs", *J. Mech. Sci. Technol.*, **26**(5), 1455-1462.
Ghorbanpour Arani, A., Atabakhshian, V., Loghman, A., Shajari, A.R. and Amir, S. (2012b), "Nonlinear vibration of embedded SWBNNTs based on nonlocal Timoshenko beam theory using DQ method", *Physica B*, **407**(13), 2549-2555.
Ghorbanpour Arani, A., Abdollahian, M., Kolahchi, R. and Rahmati, A.H. **(**2013a**)**, "Electro-thermo-torsional buckling of an embedded armchair DWBNNT using nonlocal shear deformable shell model", *Compos. Part B-ng*, **51**, 291-299.
Ghorbanpour Arani, A., Kolahchi, R. and Maraghi, Z.K. (2013b), "Nonlinear vibration and instability of embedded double-walled boron nitride nanotubes based on nonlocal cylindrical shell theory", *Appl. Math. Model.*, **37**(14-15), 7685-7707.
Griffiths, D.J. (1989), *Introduction to Electrodynamics*, (4th Ed.), Prentice Hall, Englewood Cliffs, NJ, USA.
Gurtin, M.E., Weissmüller, J. and Larché, F. (1998), "A general theory of curved deformable interfaces in solids at equilibrium", *Philos. Mag. A*, **78**(5), 1093-1109.
Hadjesfandiari, A.R. (2013), "Size-dependent piezoelectricity", *Int. J. Solids Struct.*, **50**(18), 2781-2791.
Hadjesfandiari, A.R. and Dargush, G.F. (2011), "Couple stress theory for solids", *Int. J. Solids Struct.*, **48**(18), 2496-2510.

Hadjesfandiari, A.R. and Dargush, G.F. (2013), "Fundamental solutions for isotropic size-dependent couple stress elasticity", *Int. J. Solid. Struct.*, **50**(9), 1253-1265.
Hosseini-Hashemi, S., Nahas, I., Fakher, M. and Nazemnezhad, R. (2014), "Surface effects on free vibration of piezoelectric functionally graded nanobeams using nonlocal elasticity", *Acta Mech*, **225**(6), 1555-1564.
Hummer, G., Rasaiah, J.C. and Noworyta, J.P. (2001), "Water conduction through the hydrophobic channel of a carbon nanotube", *Nature*, **414**(6860), 188-190.
Ke, L.L. and Wang, Y.S. (2012), "Thermoelectric-mechanical vibration of piezoelectric nanobeams based on the nonlocal theory", *Smart Mater. Struct.*, **21**(2), 025018.
Ke, L.L., Wang, Y.S. and Wang, Z.D. (2012), "Nonlinear vibration of the piezoelectric nanobeams based on the nonlocal theory", *Compos. Struct.*, **94**(6), 2038-2047.
Ke, L.L., Wang, Y.S., Yang, J. and Kitipornchai, S. (2014a), "The size-dependent vibration of embedded magneto-electro-elastic cylindrical nanoshells", *Struct.*, **23**(12), 1-17.
Ke, L.L., Wang, Y.S. and Reddy, J.N. (2014b), "Thermo-electro-mechanical vibration of size-dependent piezoelectric cylindrical nanoshells under various boundary conditions", *Compos. Struct.*, **116**(1), 626-636.
Kerr, A.D. (1968), "An extension of the Kantorovich method", *Q. Appl. Math.*, **26**(2), 219-229.
Koiter, W.T. (1964), "Couple stresses in the theory of elasticity", *I and II. Proc. Kon. Neder. Akad. Weten. B.*, **67**, 17-44.
Kheibari, F. and Tadi Beni, Y. (2016), "Size dependent electro-mechanical vibration of single-walled piezoelectric nanotubes using thin shell model", *Mater. Des.*, **114**, 572-583.
Lam, D.C.C., Yang, F., Chong, A.C.M., Wang, J. and Tong, P. (2003), "Experiments and theory in strain gradient elasticity", *J. Mech. Phys. Solids*, **51**(8), 1477-1508.
Lazar, M., Maugin, G.A. and Aifantis, E.C. (2005), "On dislocations in a special class of generalized elasticity", *Phys. Status Solidi B*, **242**(12), 2365-2390.
Leissa, A.W. (1993), *Vibration of Shells*, NASA, Washington, USA.
Li, A., Zhou, Sh., Zhou, Sh. and Wang, B. (2014), "Size-dependent analysis of a three-layer microbeam including electromechanical coupling", *Compos. Struct.*, **116**, 120-127.
Liang, X. and Shen, S.P. (2013), "Size-dependent piezoelectricity and elasticity due to the electric field-strain gradient coupling and strain gradient elasticity", *Int. J. Appl. Mech.*, **5**(2), 1350015-1350031.
Liu, Ch., Ke, L.L., Wang, Y.S., Yang, J. and Kitipornchai, S. (2013), "Thermo-electro-mechanical vibration of piezoelectric nanoplates based on the nonlocal theory", *Compos. Struct.*, **106**, 167-174.
Liu, J., Chen, L., Xie, F., Fan, X. and Li, Ch. (2016), "On bending, buckling and vibration of graphene nanosheets based on the nonlocal theory", *Smart Struct. Syst., Int. J.*, **17**(2), 257-274.
Loy, C.T., Lam, K.Y. and Shu, C. (1997), "Analysis of cylindrical shells using generalized differential quadrature", *Shock Vib.*, **4**(3), 193-198.
Maranganti, R., Sharma, N.D. and Sharma, P. (2006), "Electromechanical coupling in nonpiezoelectric materials due to nanoscale nonlocal size effects: Green's function solutions and embedded inclusions", *Phys. Rev. B*, **74**(1), 014110.
Markus, S. (1988), *The Mechanics of Vibrations of Cylindrical Shells*, Elsevier Science, New York, NY, USA.
Mattia, D. and Gogotsi, Y. (2008), "Review: static and dynamic behavior of liquids inside carbon nanotubes", *Microfluid Nanofluid*, **5**(3), 289-305.
Mehralian, F. and Tadi Beni, Y. (2016), "Size-dependent torsional buckling analysis of functionally graded cylindrical shell", *Compos. Part B: Eng.*, **94**, 11-25.
Mehralian, F., Tadi Beni, Y. and Ansari, R. (2016a), "Size dependent buckling analysis of functionally graded piezoelectric cylindrical nanoshell", *Compos. Struct.*, **152**, 45-61.
Mehralian, F., Tadi Beni, Y. and Ansari, R. (2016b), "On the size dependent buckling of anisotropic piezoelectric cylindrical shells under combined axial compression and lateral pressure", *Int. J. Mech. Sci.*, **119**, 155-169.
Mindlin, R.D. and Tiersten, H.F. (1962), "Effects of couple-stresses in linear elasticity", *Arch. Ration. Mech. Anal.*, **11**(1), 415-448.
Mishima, T., Fujioka, H., Nagakari, S., Kamigaki, K. and Nambu, S. (1997), "Lattice image observations of

nanoscale ordered regions in Pb (Mg1/3Nb2/3)O-3", *Jpn. J. App. Phys.*, **36**(9), 6141-6144.
Mohammadi Dashtaki, P. and Tadi Beni, Y. (2014), "Effects of Casimir force and thermal stresses on the buckling of electrostatic nano-bridges based on couple stress theory", *Arab. J. Sci. Eng.*, **39**(7), 5753-5763.
Pan, Z.W., Dai, Z.R. and Wang, Z.L. (2001), "Nanobelts of semiconducting oxides", *Science*, **291**(5510), 1947-1949.
Park, K.-I., Xu, S., Liu, Y., Hwang, G.-T., Kang, S.-J., Wang, Z.L. and Lee, K.J. (2010), "Piezoelectric BaTiO3 thin film nanogenerator on plastic substrates", *Nano Lett.*, **10**(12), 4939-4943.
Razavi, H., Faramarzi Babadi, A. and Tadi Beni, Y. (2016), "Free vibration analysis of functionally graded piezoelectr ic cylindrical nanoshell based on consistent couple stress theory", *Compos. Struct.*, **160**, 1299-1309.
Sahmani, S., Aghdam, M.M. and Akbarzadeh, A.H. (2016), "Size-dependent buckling and postbuckling behavior of piezoelectric cylindrical nanoshells subjected to compression and electrical load", *Mater. Des.* **105**, 341-351.
Sedighi, H.M. (2014), "Size-dependent dynamic pull-in instability of vibrating electrically actuated microbeams based on the strain gradient elasticity theory", *Acta Astronautica*, **95**, 111-123.
Sedighi, H.M. and Bozorgmehri, A. (2016), "Dynamic instability analysis of doubly clamped cylindrical nanowires in the presence of Casimir attraction and surface effects using modified couple stress theory", *Acta Mech.*, **227**(6), 1575-1591.
Sedighi, H.M. and Farjam, N. (2016), "A modified model for dynamic instability of CNT based actuators by considering rippling deformation, tip‐charge concentration and Casimir attraction", *Microsyst. Technol.*, 1-17.
Sedighi, H.M., Daneshmand, F. and Abadyan, M. (2015), "Dynamic instability analysis of electrostatic functionally graded doubly-clamped nano-actuators", *Compos. Struct.res*, **124**, 55-64.
Shayan-Amin, S., Dalir, H. and Farshidianfar, A. (2009), "Molecular dynamics simulation of double-walled carbon nanotube vibrations: Comparison with continuum elastic theories", *J. Mech.*, **25**(4), 337-343.
Shojaeian, M. and Tadi Beni, Y. (2015), "Size-dependent electromechanical buckling of functionally graded electrostatic nano-bridges", *Sensors Actuators A: Physical*, **232**, 49-62.
Shojaeian. M., Tadi Beni, Y. and Ataei, H. (2016a), "Electromechanical buckling of functionally graded electrostatic nanobridges using strain gradient theory", *Acta Astronautica*, **118**, 62-71.
Shojaeian, M., Tadi Beni, Y. and Ataei, H. (2016b), "Size-dependent snap-through and pull-in instabilities of initially curved pre-stressed electrostatic nano-bridges", *J. Phys. D: Appl. Phys.*, **49**(29), 295-303.
Shvartsman, V.V., Emelyanov, A.Y., Kholkin, A.L. and Safari, A. (2002), "Local hysteresis and grain size effects in Pb(Mg1/3Nb2/3)O-SbTiO3", *Appl. Phys. Lett.*, **81**(1), 117-119.
Tadi Beni, Y. (2016a), "A nonlinear electro-mechanical analysis of nanobeams based on the size-dependent piezoelectricity theory", *J. Mech.*, **65**, 1-13.
Tadi Beni, Y. (2016b), "Size-independent electromechanical bending, buckling, and free vibration analysis of functionally graded piezoelectric nanobeams", *J. Intellig. Mater. Syst. Struct.*, **27**, 2199-2215.
Tadi Beni, Y. (2016c), "Size-dependent analysis of piezoelectric nanobeams including electro-mechanical coupling", *Mech. Res. Commun.*, **75**, 67-80.
Tadi Beni, Y. and Abadyan, M. (2013), "Size-dependent pull-in instability of torsional nano-actuator", *Physica Scripta*, **88**(5), 55801-55810.
Tadi Beni, Y. and Zeighampour, H. (2014a), "Cylindrical thin-shell model based on modified strain gradient theory", *Int. J. Eng. Sci.*, **78**, 27-47.
Tadi Beni, Y. and Zeighampour, H. (2014b), "Analysis of conical shells in the framework of coupled stresses Theory", *Int. J. Eng. Sci.nce*, **81**, 107-122.
Tadi Beni, Y., Abadyan, M.R. and Noghrehabadi, A. (2011), "Investigation of Size Effect on the Pull-in Instability of Beamtype NEMS under van der Waals Attraction", *Procedia Eng.*, **10**, 1718-1723.
Tadi Beni, Y., Koochi, A. and Abadyan, M.R. (2014), "Using modified couple stress theory for modeling the size dependent pull-in instability of torsional nano-mirror under Casimir force", *Int. J. Optomechatron.*, **8**(1), 47-71.

Tsai, J.-L. and Tu, J.-F. (2010), "Characterizing mechanical properties of graphite using molecular dynamics simulation", *Mater. Des*, **31**(1), 194-199.
Toupin, R.A. (1962), "Elastic materials with couple-stresses", *Arch. Ration. Mech. Anal.*, **11**(1), 385-414.
Voigt, W. (1887), "Theoretische Studien fiber die Elastizitatsverhiltnisse der Kristalle [Theoretical studies on the elasticity relationships of crystals]" In: *Abhandlungen zur Geschichte der mathematischen Wissenschaften*, Springer, p. 34.
Wang, Z.L. (2009), "ZnO nanowire and nanobelt platform for nanotechnology", *Mater. Sci. Eng. R.*, **64**(3-4), 33-71.
Wang, G.-F., Yu, S.-W. and Feng, X.-Q. (2004), "A piezoelectric constitutive theory with rotation radient effects", *Eur, J. Mech. A Solid*, **23**(3), 455-466.
Xu, S. and Wang, Z.L. (2011), "One-dimensional ZnO nanostructures: solution growth and functional properties (invited review)", *Nano Res.*, **4**(11), 1013-1098.
Yang, F., Chong, A.C.M., Lam, D.C.C. and Tong, P. (2002), "Couple stress based strain gradient theory for elasticity", *Int. J. Solids Struct.*, **39**(10), 2731-2743.
Zeighampour, H. and Tadi Beni, Y. (2014), "A shear deformable cylindrical shell model based on couple stress theory", *Arch Appl. Mech.*, **85**(4), 539-553.
Zeighampour, H. and Tadi Beni, Y. (2015), "Free vibration analysis of axially functionally graded nanobeam with radius varies along the length based on strain gradient theory", *Appl. Math. Model.*, **39**(18), 5354-5369.
Zhao, M.-H., Wang Z.-L. and Mao S.X. (2004), "Piezoelectric characterization of individual zinc oxide nanobelt probed by piezoresponse force microscope", *Nano Lett.*, **4**(4), 587-590.

CC

Appendix A

In equations of motion (23)-(28), The constant coefficents $A_1 - A_{12}$, $B_1 - B_{17}$, $C - C$, $D_1 - D_{14}$, $E_1 - E_{16}$, $F_1 - F_8$ are expressed as follows

$$A_1 = -\frac{Eh}{1-\nu^2}, A_2 = \frac{\mu h l^2}{R^2}, A_3 = -\frac{\mu h}{R^2}, A_4 = \frac{\mu h l^2}{R^4}, A_5 = -\frac{\mu h l^2}{R},$$
$$A_6 = -\frac{Eh\nu}{R(1-\nu^2)} - \frac{\mu h}{R} + \frac{\mu h l^2}{R^3}, \mathrm{A}_7 = -\frac{\mu h l^2}{R^3}, A_8 = -\frac{Eh\nu}{R(1-\nu^2)}, A_9 = -\frac{2\mu h l^2}{R^3}, \tag{A1}$$
$$A_{10} = \frac{\mu h l^2}{R^2}, \mathrm{A}_{11} = \frac{\mu h l^2}{R^3}$$

$$B_1 = \mu h l^2, B_2 = -\mu h + \frac{\mu h l^2}{R^2}, B_3 = -\frac{Eh}{R^2(1-\nu^2)} - \frac{\mu h l^2}{R^4}, B_4 = \frac{\mu h l^2}{R^2},$$
$$B_5 = \frac{k_s \mu h}{R^2} - \frac{\mu h l^2}{R^4}, B_6 = -\frac{\mu h l^2}{R}, B_7 = -\frac{\mu h l^2}{R^3}, B_8 = -\frac{Eh\nu}{R(1-\nu^2)} - \frac{\mu h}{R} + \frac{\mu h l^2}{R^3},$$
$$B_9 = \frac{3\mu h l^2}{R^2}, B_{10} = \frac{\mu h l^2}{R^4}, B_{11} = -\frac{Eh}{R^2(1-\nu^2)} + \frac{\mu h l^2}{R^4} - \frac{k_s \mu h}{R^2}, B_{12} = -\frac{2\mu h l^2}{R^2}, \tag{A2}$$
$$B_{13} = -\frac{\mu h l^2}{R^3}, B_{14} = -\frac{k_s \mu h}{R} - \frac{\mu h l^2}{R^3}, B_{15} = -\frac{\mu h l^2}{R}, \mathrm{B}_{16} = -\frac{2fh}{\pi R^3},$$

$$\mathrm{C}_1 = \mu h l^2, \mathrm{C}_2 = -k_s \mu h - \frac{\mu h l^2}{R^2}, \mathrm{C}_3 = \frac{2\mu h l^2}{R^2}, \mathrm{C}_4 = \frac{\mu h l^2}{R^4}, \mathrm{C}_5 = -\frac{k_s \mu h}{R^2} - \frac{\mu h l^2}{R^4},$$
$$\mathrm{C}_6 = \frac{Eh}{R^2(1-\nu^2)}, \mathrm{C}_7 = \frac{Eh\nu}{R(1-\nu^2)}, \mathrm{C}_8 = \frac{2\mu h l^2}{R^3}, \mathrm{C}_9 = \frac{2\mu h l^2}{R^2},$$
$$\mathrm{C}_{10} = \frac{Eh}{R^2(1-\nu^2)} + \frac{k_s \mu h}{R^2} + \frac{\mu h l^2}{R^4} \mathrm{C}_{11} = -\frac{\mu h l^2}{R^4}, \mathrm{C}_{12} = -\frac{\mu h l^2}{R^2}, \mathrm{C}_{13} = -\mu h l^2, \tag{A3}$$
$$\mathrm{C}_{14} = -k_s \mu h + \frac{\mu h l^2}{R^2}, \mathrm{C}_{15} = -\frac{\mu h l^2}{R^3}, \mathrm{C}_{16} = -\frac{k_s \mu h}{R} + \frac{\mu h l^2}{R^3},$$
$$\mathrm{C}_{17} = -\frac{\mu h l^2}{R}, \mathrm{C}_{18} = \frac{2fh}{\pi R}, \mathrm{C}_{19} = -\frac{2fh}{\pi R^3},$$

$$D_1 = -\frac{Eh^3}{12(1-\nu^2)} - \mu h l^2, D_2 = \frac{\mu h^3 l^2}{12R^2}, D_3 = \frac{\mu h^3 l^2}{12R^4}, D_4 = -\frac{\mu h^3}{12R^2}, \tag{A4}$$

$$D_5=\frac{\mu hl^2}{R^2}+k_s\mu h, D_6=-\frac{\mu h^3}{12R}-\frac{Eh^3\nu}{12R(1-\nu^2)}-\frac{\mu hl^2}{R}, D_7=-\frac{\mu h^3l^2}{12R^3},$$
$$D_8=-\frac{\mu h^3l^2}{12R}, D_9=\frac{\mu hl^2}{R^3}, D_{10}=\frac{2\mu hl^2}{R^2}, D_{11}=\mu hl^2, D_{12}=\frac{\mu hl^2}{R^2}, \quad \text{(A4)}$$
$$D_{13}=\frac{\mu hl^2}{R^2}+k_s\mu h, D_{14}=\frac{2fh}{\pi R},$$

$$E_1=\frac{\mu h^3l^2}{12}, E_2=-\frac{\mu h^3}{12}, E_3=\frac{\mu h^3l^2}{12R^2}, E_4=-\frac{\mu h^3l^2}{12R^4}-\frac{Eh^3}{12R^2(1-\nu^2)}-\frac{\mu h l^2}{R},$$
$$E_5=\frac{\mu hl^2}{R^2}+k_s\mu h, E_6=-\frac{\mu h^3}{12R}-\frac{Eh^3\nu}{12R(1-\nu^2)}-\frac{\mu hl^2}{R}, E_7=-\frac{\mu h^3l^2}{12R^2},$$
$$E_8=-\frac{\mu h^3l^2}{12R^2}, E_9=\frac{\mu hl^2}{R^2}, E_{10}=-\frac{\mu hl^2}{R}, E_{11}=-\frac{\mu hl^2}{R^3}, E_{12}=\frac{\mu hl^2}{R^3}-\frac{k_s\mu h}{R}, \quad \text{(A5)}$$
$$E_{13}=\frac{\mu hl^2}{R}, E_{14}=\frac{\mu hl^2}{R^3}, E_{15}=-\frac{\mu hl^2}{R^3}+\frac{k_s\mu h}{R}, E_{16}=-\frac{2fh}{\pi R^2},$$

$$F_1=\frac{\varepsilon h}{2}, F_2=\frac{\varepsilon h}{2R^2}, F_3=\frac{\varepsilon\pi^2}{2h}, F_4=\frac{2fh}{\pi R^3}, F_5=-\frac{2fh}{\pi R}, F_6=\frac{2fh}{\pi R^2},$$
$$\mathrm{F}_7=\frac{2fh}{\pi R}, F_8=-\frac{2fh}{\pi R^3} \quad \text{(A6)}$$

Appendix B

In boundry conditions Eqs. (29)-(46), The constant coefficents $a_1^1-a_8^1$, $b_1^1-b_{15}^1$, $c_1^1-c_{14}^1$, $d_1^1-d_5^1$, $e_1^1-e_7^1$, $f_1^1-f_5^1$ and $a_1^2-a_{14}^2$, $b_1^2-b_{11}^2$, $c_1^2-c_{16}^2$, $d_1^2-d_7^2$, $e_1^2-e_7^2$, $f_1^2-f_6^2$ are expressed as follows

$$a_1^1=\frac{Eh}{1-\nu^2}, \mathrm{a}_2^1=-\frac{\mu hl^2}{R^2}, \mathrm{a}_3^1=\frac{\mu hl^2}{R}, \mathrm{a}_4^1=\frac{Eh\nu}{R(1-\nu^2)}-\frac{\mu hl^2}{R^3}, a_5^1=\frac{Eh\nu}{R(1-\nu^2)},$$
$$\mathrm{a}_6^1=\frac{\mu hl^2}{R^3}, \mathrm{a}_7^1=-\frac{\mu hl^2}{R^2}, a_8^1=\frac{2fh}{\pi R^2}, \quad \text{(B1)}$$

$$b_1^1=-\mu hl^2, \mathrm{b}_2^1=\mu h+\frac{\mu hl^2}{R^2}, \mathrm{b}_3^1=-\frac{\mu hl^2}{R^2}, \mathrm{b}_4^1=\frac{\mu hl^2}{R}, \mathrm{b}_5^1=\frac{\mu hl^2}{R^3}, \quad \text{(B2)}$$

$$\begin{gathered}
\mathrm{b}_6^1=\frac{\mu h}{R},\mathrm{b}_7^1=-\frac{2\mu hl^2}{R^2},\mathrm{b}_8^1=\frac{\mu hl^2}{R^2},b_9^1=\frac{\mu hl^2}{R},b_{10}^1=\mu hl^2,b_{11}^1=-\frac{\mu hl^2}{R^2},\\
b_{12}^1=-\frac{\mu hl^2}{R},b_{13}^1=\frac{\mu hl^2}{R^2},b_{14}^1=-\frac{\mu hl^2}{R},b_{15}^1=\frac{2fh}{\pi R},
\end{gathered} \tag{B2}$$

$$\begin{gathered}
c_1^1=-\mu hl^2,\mathrm{c}_2^1=\mu h+\frac{\mu hl^2}{R^2},\mathrm{c}_3^1=-\frac{\mu hl^2}{R^2},\mathrm{c}_4^1=-\frac{\mu hl^2}{R^3},\mathrm{c}_5^1=\frac{2\mu hl^2}{R^2},\\
\mathrm{c}_6^1=\mu h-\frac{\mu hl^2}{R^2},\mathrm{c}_7^1=\mu hl^2,c_8^1=\frac{\mu hl^2}{R},\mathrm{c}_9^1=-\frac{2fh}{\pi R},c_{10}^1=\mu hl^2,\mathrm{c}_{11}^1=\frac{\mu hl^2}{R^2},\\
\mathrm{c}_{12}^1=-\frac{\mu hl^2}{R},\mathrm{c}_{13}^1=\mu hl^2,\mathrm{c}_{14}^1=-\frac{\mu hl^2}{R^2},
\end{gathered} \tag{B3}$$

$$\begin{gathered}
d_1^1=-\mu hl^2,\mathrm{d}_2^1=-\frac{\mu hl^2}{R^2},\mathrm{d}_3^1=\frac{Eh^3\nu}{12R(1-\nu^2)}+\frac{\mu hl^2}{R},\\
\mathrm{d}_4^1=\frac{Eh^3}{12(1-\nu^2)}+\mu hl^2,\mathrm{d}_5^1=\frac{\mu h\,\hat{l}}{R^2}d_6^1=\frac{\mu h^3l^2}{12R},\mathrm{d}_7^1=-\frac{\mu h^3l^2}{12R^2},
\end{gathered} \tag{B4}$$

$$\begin{gathered}
e_1^1=\frac{\mu h^3}{12},e_2^1=\frac{\mu h^3}{12R},e_3^1=\frac{\mu h^3l^2}{12R^3},e_4^1=\frac{\mu h^3l^2}{12R},e_5^1=-\frac{\mu h^3l^2}{12},e_6^1=-\frac{\mu h^3l^2}{12R^2},\\
e_7^1=-\frac{\mu h^3l^2}{12R},e_8^1=\frac{\mu h^3l^2}{12}
\end{gathered} \tag{B5}$$

$$f_1^{\,1}=-\frac{\varepsilon h}{2},f_2^{\,1}=-\frac{2fh}{\pi R},f_3^{\,1}=\frac{2fh}{\pi R^2},f_4^{\,1}=-\frac{2fh}{\pi R},f_5^{\,1}=\frac{2fh}{\pi R}, \tag{B6}$$

$$\begin{gathered}
a_1^2=-\frac{\mu hl^2}{R^4},\mathrm{a}_2^2=\frac{\mu h}{R^2},\mathrm{a}_3^2=-\frac{\mu hl^2}{R^2},\mathrm{a}_4^2=\frac{\mu hl^2}{R^3},a_5^2=\frac{\mu h}{R}-\frac{\mu hl^2}{R^3},\\
\mathrm{a}_6^2=\frac{\mu hl^2}{R},\mathrm{a}_7^1=\frac{2\mu hl^2}{R^3},a_8^2=-\frac{\mu hl^2}{R^3},\mathrm{a}_9^2=-\frac{\mu hl^2}{R^2},a_{10}^2=\frac{\mu hl^2}{R^4},\\
\mathrm{a}_{11}^2=-\frac{\mu hl^2}{R^3},a_{12}^2=-\frac{\mu hl^2}{R^3},a_{13}^2=-\frac{\mu hl^2}{R^3},\mathrm{a}_{14}^2=\frac{2fh}{\pi R^2},
\end{gathered} \tag{B7}$$

$$b_1^2=\frac{Eh}{R^2(1-\nu^2)}+\frac{\mu hl^2}{R^4},\mathrm{b}_2^2=-\frac{\mu hl^2}{R^2},\mathrm{b}_3^2=\frac{\mu hl^2}{R^3},\mathrm{b}_4^2=\frac{Eh\nu}{R(1-\nu^2)}, \tag{B8}$$

$$b_5^2=\frac{Eh}{R^2(1-\nu^2)},b_6^2=-\frac{\mu hl^2}{R^4}b_7^2=\frac{\mu hl^2}{R^3},\mathrm{b}_8^2=\frac{2\mu hl^2}{R^2},\mathrm{b}_9^2=-\frac{\mu hl^2}{R^2},$$
$$b_{10}^2=-\frac{\mu hl^2}{R^2},\mathrm{b}_{11}^2=\frac{2fh}{\pi R}, \tag{B8}$$

$$c_1^2=-\frac{\mu hl^2}{R^4},\mathrm{c}_2^2=\frac{\mu h}{R^2}+\frac{\mu hl^2}{R^4},\mathrm{c}_3^2=-\frac{\mu hl^2}{R^2},\mathrm{c}_4^2=\frac{\mu hl^2}{R^2},\mathrm{c}_5^2=\frac{\mu hl^2}{R^4},$$
$$\mathrm{c}_6^2=-\frac{\mu h}{R^2}-\frac{\mu hl^2}{R^4},\mathrm{c}_7^2=-\frac{\mu hl^2}{R^3},c_8^2=\frac{\mu hl^2}{R^2},c_9^2=\frac{\mu h}{R}-\frac{\mu hl^2}{R^3},$$
$$\mathrm{c}_{10}^2=\frac{\mu hl^2}{R^3},\mathrm{c}_{11}^2=\frac{2fh}{\pi R^3},c_{12}^2=-\frac{\mu hl^2}{R^4},\mathrm{c}_{13}^2=\frac{\mu hl^2}{R^2},\mathrm{c}_{14}^2=\frac{\mu hl^2}{R^4},$$
$$\mathrm{c}_{15}^2=-\frac{\mu hl^2}{R^2},\mathrm{c}_{16}^2=-\frac{\mu hl^2}{R^3}, \tag{B9}$$

$$\mathrm{d}_1^2=-\frac{\mu h^3l^2}{12R^4},d_2^2=\frac{\mu h^3}{12R},\mathrm{d}_3^2=\frac{\mu h^3l^2}{12R^3},\mathrm{d}_4^2=\frac{\mu h^3l^2}{12R},$$
$$\mathrm{d}_5^2=-\frac{\mu h^3l^2}{12R^2},\mathrm{d}_6^2=\frac{\mu h^3l^2}{12R^4},\mathrm{d}_7^2=-\frac{\mu h^3l^2}{12R^3}, \tag{B10}$$

$$e_1^2=\frac{\mu hl^2}{R^3},e_2^2=-\frac{\mu hl^2}{R},e_3^2=-\frac{\mu hl^2}{R^3},e_4^2=\frac{Eh^3\nu}{12(1-\nu^2)R}+\frac{\mu hl^2}{R},e_5^2=\frac{\mu h^3l^2}{R^3},$$
$$e_6^2=\frac{Eh^3}{12(1-\nu^2)R^2}+\frac{\mu h\ \dot{l}^2}{R^2}+\frac{\mu h^3l^2}{12R^4},e_7^2=-\frac{\mu h^3l^2}{12R^2}, \tag{B11}$$

$$f_1^{\ 2}=-\frac{\varepsilon h}{2R^2},f_2^{\ 1}=\frac{2fh}{\pi R},f_3^{\ 1}=\frac{2fh}{\pi R^4},f_4^{\ 1}=-\frac{2fh}{\pi R^2},f_5^{\ 1}=-\frac{2fh}{\pi R^4},f_6^{\ 1}=-\frac{2fh}{\pi R^2} \tag{B12}$$